MASTER

A convenient internal numbering-up strategy for the scale up of gas-liquid photoredox catalysis

Kuijpers, Koen P.L.

Award date:
2016

Technische Universiteit
Eindhoven
University of Technology

Process Engineering
Micro Flow Chemistry and Process Technology (SCR-SFP)
Department of Chemical Engineering and Chemistry
Helix building, Het Kranenveld 14
P.O. Box 513, 5600 MB Eindhoven
The Netherlands
www.tue.nl

A convenient internal numbering-up strategy for the scale up of gas-liquid photoredox catalysis

Koen Kuijpers

August 2015

Daily supervisor
Dr. Yuanhai Su

Supervisor
Dr. T. Noël

Graduation Professor
Prof. Dr. V. Hessel

External committee member
Dr. ir. J.T. Padding

Abstract

As microreactor technology still faces throughput limitations, therefore this study focusses on scale-up via numbering up of microchannels to overcome these challenges. Two types of reactors are tested: a multichannel micromixer and a self-designed flexible capillary reactor. The latter reactor allows to measure outputs for each channel separately. A hydrodynamic study is done in order to determine the equality of the flows amongst the channels. Also a model reaction is applied to test the scale-up possibilities for photoredox catalyzed reaction systems. As model reaction the formation of phenyl disulfide from thiophenol with Eosin Y as homogeneous catalyst is selected.

Experiments with the multichannel micromixer show that photocatalytic reactions are not applicable in this device, because flow patterns for multiphase flow – in this study liquid-liquid two phase flow and gas-liquid flow – only appeared to be stable at very high flowrates with residence times of less than one second. In contrast to the multichannel micromixer, the self-designed reactor showed to be highly applicable for photocatalysis. The hydrodynamic study showed that numbering-up could be implemented with less than 5 percent deviation in liquid throughput among 8 reactor channels. Implementation of the model reaction confirmed its promising application for scale-up, via numbering-up, of photocatalysis with a deviation in yield of less than 5 percent and a deviation in throughput of less than 10 percent. Furthermore, quantum yield of the reaction is determined and mechanism of the formation of phenyl disulfide from thiophenol with Eosin Y as photocatalyst is proposed.

Contents

Chapter 1

Introduction

Currently, because of depleting resources and increasing consciousness of exhaust gasses, process intensification and new reactor concepts are gaining great attention. One way of realizing these novel concepts is proposed by Hessel in the Novel Process Windows concept. In this concept microreactors are suggested to be a promising novel reactor concept, due to their small dimensions (typically 100-1000 μm internal diameter and a volume of several hundreds of μL) and high surface-to-volume ratios they possess superior mass and heat transfer capacities compared to conventional reactor concepts. The Novel Process Windows concept indicates 6 main routes of process intensification, as showed in Figure 1: high concentrations or solvent free reactions, elevated temperature and pressure, new chemical transformation possibilities, reactions in the explosive regime and process simplification & integration[1].

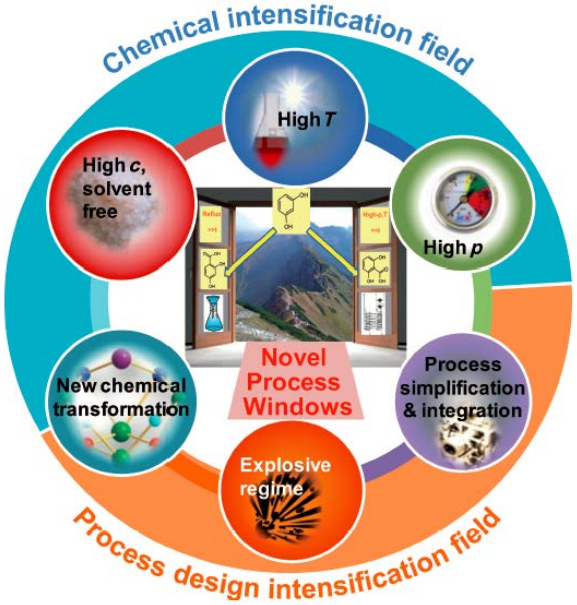

Figure 1: A schematic representation of the Novel Process Window concept[1]

Photochemistry in microflow

The world's energy consumption is increasing thus scientists focus more on energy efficiency. Light is an inexpensive and widely available source of energy. In particular, recent advances in photocatalysts lead to the rapid evolution visible light photocatalysis as an alternative with high application potential compared to traditional reaction pathways. Chemical reactions require to overcome an energy barrier, which in many reactions can be satisfied by the energy made available through light. Photochemistry is an alternative to activate reactions with light and is therefore an alternative for elevated temperatures and pressures, making it a greener activation

pathway. It also opens new reaction pathways that are challenging to reach through thermochemical transformations[2].

Multiple factors are involved in the efficiency of photocatalysis such as light absorption and redox potentials. The efficiency of photons in a reactor largely depends on the light absorbance of the reaction medium. As can be seen in Equation (1). the absorption is determined via the Bouguer-Lambert-Beer law, which states that the absorbance (A) is a function of the transmittance (T) and depends on the molar extinction coefficient (ε), the molar concentration and the path length of the light (l) penetrating the reaction medium.

$$A = \log_{10}\left(T_\lambda\right) = \log_{10}\left(\frac{I}{I_0}\right) = \varepsilon_\lambda \cdot C_\lambda \cdot l_\lambda \tag{1}$$

Microreactors can provide a great advantage in photochemistry with their small dimensions (short transport distances), which are typically in the order of micrometers or even smaller. A smaller channel enables a shorter path length and therefore enhances reaction efficiency. Of course it should be noted that the microreactor has to be transparent in order to allow irradiation of the reaction medium. When working with a gas-liquid system microreactors hold even more advantages such as good mixing properties, compared to other flow regimes (e.g. bubble flow and churn flow). In Taylor flow (segmented flow) gas and liquid slug are alternating and the gas bubble is surrounded by a thin liquid film. In the liquid slugs, mixing is enhanced by vortexes caused by internal friction and slip velocity. This phenomenon results in homogeneous mixing and improves mass transfer rates between the gas and liquid phase. Because Taylor flow is characterized by minimal axial dispersion this system can be assumed to behave as ideal plug flow[3]. This statement is backed by values of the capillary number in the order of 10^{-3} and according ideal plug flow[4].

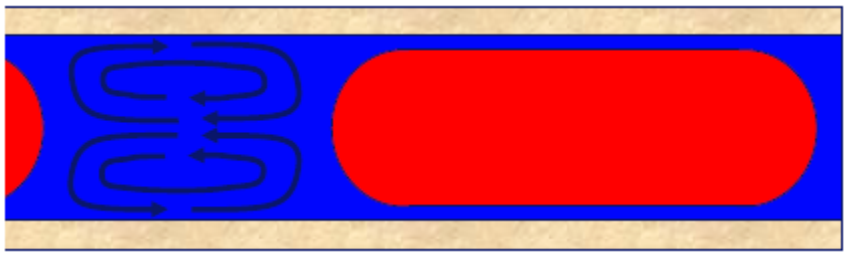

Figure 2: Image of Taylor flow and internal circulations within a liquid slug[5]

For gas-liquid and liquid-liquid systems, the reaction can be evaluated via a dimensionless parameter called the Hatta number (Ha), which compares the reaction rate in the liquid film around gas phase (e.g. gas bubbles) with the diffusion rate through this film. The Hatta number for a reaction with *m*th order of reactant A and *n*th order of reactant B is stated in Equation (2), where A represents the discontinuous phase. In this equation $k_{m,n}$ is the reaction rate constant, $C_{A,i}$ is the concentration of species A at the interface, $C_{B,bulk}$ is the concentration of species B in the bulk phase, D_A is the molecular diffusivity and k_L represents the mass transfer coefficient.

$$Ha = \frac{\sqrt{\frac{2}{m+1} k_{m,n} (C_{A,i})^{m-1} (C_{B,bulk})^n D_A}}{k_L} \tag{2}$$

The evaluated multiphase reactions can be divided into three categories: Ha<0.3, 0.3<Ha<3, Ha>3. When Ha<0.3, it indicates a slow reaction regime or reaction in the bulk phase. In this case, there are no mass transfer limitations in reaction processes; whereas, if Ha>3, the reaction occurs at the interface of gas-liquid two phases, indicating a fast reaction regime or a mass transfer limited regime.

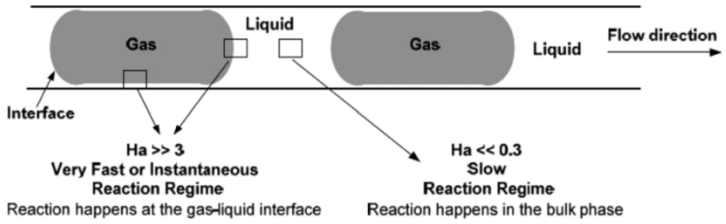

Figure 3: Schematic representation of different reaction regimes in Taylor flow evaluated by the Hatta number

In addition to the high transport rates, microreactors provide the possibility for application of previously uncontrollable reactions[1,6]. Also, photochemical reactions can be done under non-harsh conditions[7] (e.g. room temperature, atmospheric pressure). The combination of photochemistry with microreactor technology provides a strong tool for discovering reaction mechanisms, showing large application potential on accurate drug delivery[8], vitamin production[9] as well as for the degradation of viruses, bacteria and pharmaceuticals[10].

Research aims

Microreactors currently still face some issues such as their small throughput. While for single-phase operation, both gas and liquid, suitable concepts are at hand and have let here and there to entering industrial production, this is more difficult for gas-liquid and especially photocatalytic microreactors. Thus, good scale-up concepts are still to be developed here. This is because the most efficient approach, which is smart scale-out (in internal dimensions) does not work well here for reasons given below (in Chapter 2.1). Thus, the main focus needs to be on the numbering-up approach to scale-up microreactors. This generally is a promising technique for industry as it is a possibility to increase production capacity up to industrial standards while maintaining the advantages of the microscale reactors, such as high heat and mass transfer rates. However, good distribution among the channels in an internal numbered-up system is difficult to establish and this

holds even more for a gas-liquid flowing system. This study presents a convenient method for internal numbering-up a microreactor for a heterogeneous gas-liquid system in the slug flow regime. Next to the hydrodynamics, this study will further extend to heterogeneous gas-liquid photoreaction processes: the photocatalytic oxidation of thiophenol with oxygen using the photocatalyst Eosin Y under visible light illumination, as can be seen in Figure 4. Whereas the conventional way of establishing these disulfide bonds includes metal catalysts, the photocatalytic process uses an organic dye (Eosin Y). This photocatalytic formation of disulfide bonds can be done under mild conditions, which can be easily implemented. This reaction has already successfully been proven under ambient conditions in the Micro Flow Chemistry & Process Technology group[11] in Eindhoven University of Technology. High yield is obtained and with the use of continuous-flow photomicroreactor reaction time is significantly reduced from 16 hours in batch to 20 minutes in flow.

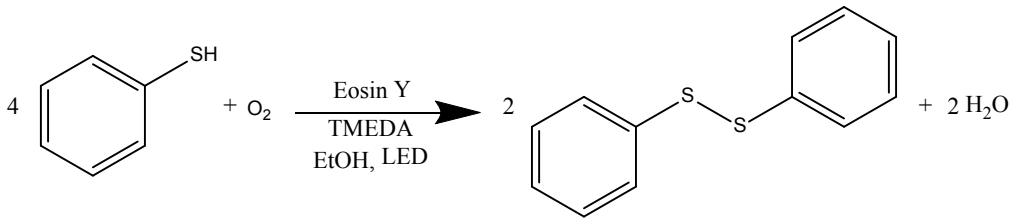

Figure 4: Disulfide formation reaction scheme

Moreover, for this heterogeneous gas-liquid system a kinetic study is performed on this reaction in previous research[12]. The kinetic rate constant was determined in a totally mass transfer free zone. A first order in thiophenol has been found for this reaction system. Equation (3) represents the firsts order in thiophenol, assumed that the liquid is saturated with oxygen. That is, the concentration of oxygen in liquid phase is kept constant during reaction process due to excessive supply of oxygen and fast mass transfer rate of oxygen from the gas to the liquid phase. Integration of Equation (3) will give Equation (4), where the conversion (X) equals the yield (Y) due to 100% selectivity of the reaction. When the natural logarithm is then plotted versus the residence time (τ) the kinetic rate constant ($K_{thiophenol}$) can be obtained: this constant is obtained with a accuracy of over 99% for a first order in thiophenol[12].

$$r_{thiophenol} = -\frac{dC_{thiophenol}}{dt} = k_{thiophenol,1} C_{thiophenol} \tag{3}$$

$$\ln\left(\frac{C_{thiophenol,0}}{C_{thiophenol}}\right) = \ln\left(\frac{C_{thiophenol,0}}{C_{thiophenol}(1-X_{thiophenol})}\right) = \ln\left(\frac{C_{thiophenol,0}}{C_{thiophenol}(1-Y)}\right) = k_{thiophenol,1}\tau \tag{4}$$

The reaction performance in a single capillary photomicroreactor and multi-capillary photomicroreactor systems will be compared in order to understand the interaction of hydrodynamics, mass transfer and reaction processes in the numbering-up process of capillary microreactors for heterogeneous gas-liquid photocatalytic systems.
Finally, two reactor types will be compared: a chip reactor (multichannel micromixer) and the previous mentioned self-designed capillary system.

Chapter 2

Theory and problem statement

2.1 Numbering-up

The main problem that is challenging for (photo)microreactors is the low throughput compared to industrial standards. Therefore, scaling up is necessary to make photochemistry applicable for production scale. Scale-up can be divided in three main strategies: increasing throughput, scale-out by enlarging reactor dimensions and numbering-up[13,14]. The first strategy involves making the microreactor longer and superficial velocity larger, while keeping the residence time constant. Higher superficial velocity can change hydrodynamics and transport properties. This can improve mixing and heat transfer to a certain extent. However, this method will result in higher pressure drop and thus higher energy consumption. In addition, clogging more easily occurs in very long microreactors. Secondly, increasing the dimensions of photomicroreactors will significantly lower mass and heat transfer and more importantly photon distribution in the reaction medium will deteriorate according to the Bouguer-Lamber-Beer law. Therefore it is a less favorable option for scale-up. Operating multiple microreactors in parallel, so-called numbering-up, can provide a promising solution to overcome throughput hurdles. Two main numbering-up strategies can be distinguished: external and internal numbering-up. Examples of external and internal numbering-up are shown in Figure 5. Whereas external numbering-up involves multiple autonomous reaction systems (e.g. pumps, mass flow controllers, reactor channels) in parallel, internal numbering-up typically only uses one pump and mass flow controller for gas-liquid reaction systems by splitting up the flow(s). The latter strategy diminishes the amount of equipment needed and decreases overall system volume compared to external numbering-up, making it more economically feasible. Internal numbering-up also faces an obstacle in proper distribution of the flow(s).

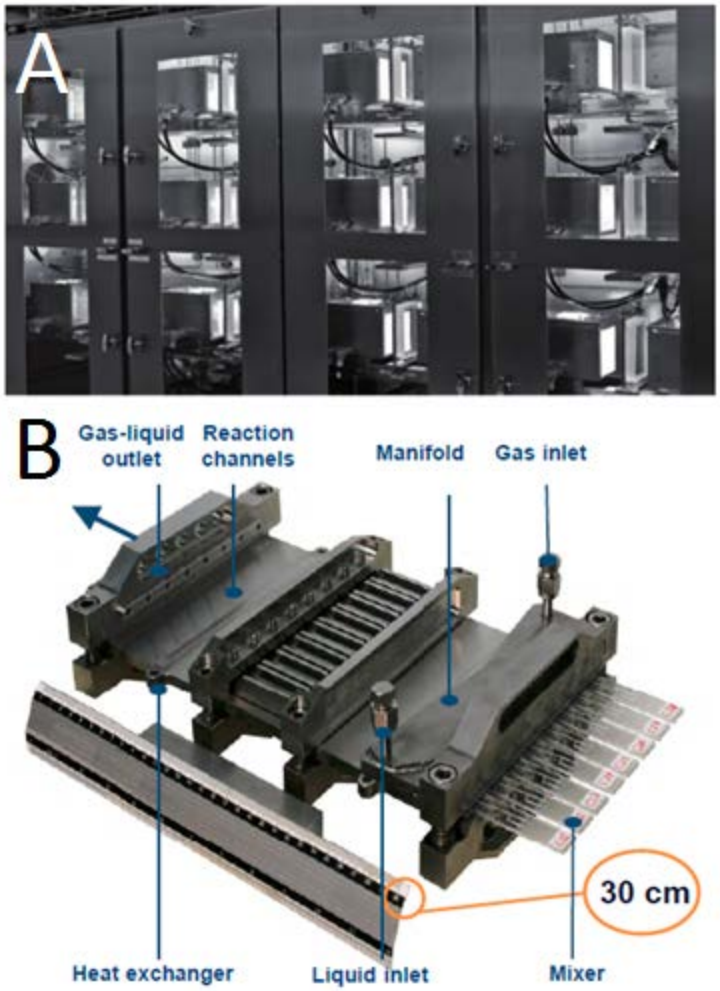

Figure 5: A) External numbering-up in a photochemical production unit by Heraeus Noblelight GmbH[2], B) Internal numbering-up in a barrier-based micro/millireactor with manifold distributor[15,16].

In order to split up streams from one inlet into multiple reactor channels, distributors have to be used. Distributors with bifurcation configurations have been proven to be highly feasible and efficient in the internal numbering-up of micro-channels for homogeneous (single-phase) mixing processes[17,18]. Also numbering-up of immiscible liquid-liquid two-phase flow systems; which are for example important in solvent extraction, reactive extraction, polymerization and other fast or instantaneous liquid–liquid heterogeneous reactions; have been studied[19–21]. Furthermore, research has been done on mass transfer[22] and flow patterns[23] as well as on the effect of surfactants on these flow patterns[24]. However, currently little is known about bifurcation distributors for gas-liquid processes and especially whether the corresponding numbering-up strategy is applicable for heterogeneous gas-liquid photochemical processes. Research on flow splitting or breakup with unsymmetrical microscale branches[25–27] has been done. However, symmetrical split-up would be better applicable in industry due to smaller differences in pressure drops, leading to better flow distribution and thus higher reaction performance when this strategy is applied in reaction processes. As indicated in literature, hydrodynamics on gas-liquid split-up for symmetrical branches was researched[15,28,29],

nonetheless difficulties with a good flow distribution was encountered due to the uncontrolled design of distributors. In a multiple microchannel system they could establish a flow non-uniformity of 10% or even more.
As mentioned in the introduction little is known about numbering-up for gas-liquid systems, especially for photochemical reaction systems. Fortunately, Al-Rawashdeh et al. provided a design theory through mathematic deduction, with which a good flow distribution could be achieved in a numbered-up microchannel reactor system[30].

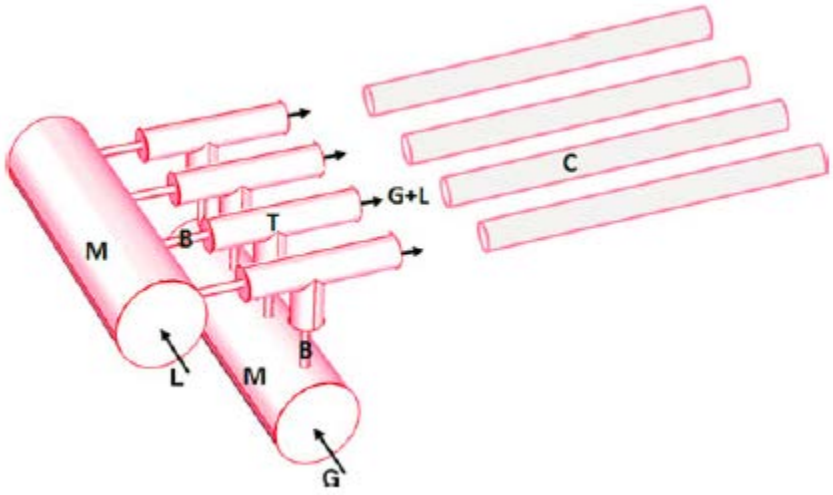

Figure 6: Reactor concept used by Al-Rawashdeh et al. Symbols used: (G) gas, (L) liquid, (M) manifold, (B) barrier channel and (T) T-mixer[30]

In this research they found that flow distribution is controlled by the pressure drop difference among the different channels. They also found that the ratio of the pressure drop of the distributor (B) part to the pressure drop in the reactor channels (C) plays a great role in the distribution. If this relative pressure drop ($\Delta\widetilde{P}$), stated in Equation (5), is high enough, 4-25 in their study, proper distribution is obtained with flow non-uniformities of 10 percent or less.

$$\Delta\widetilde{P} = \frac{\overline{P}_B}{\overline{P}_C} \tag{5}$$

Furthermore, they also tested a reaction system: phenylacetylene hydrogenation over $[Rh(NBD)(PPh_3)_2]BF_4$ catalyst. Their results show ±10 percent deviation of the numbered-up reactor compared to the single reactor system[31]. This research is used as a benchmark for this thesis.

2.3 Problem statement

Little is known about numbering-up in heterogeneous gas-liquid systems. To achieve a good flow distribution in the numbering-up process is still a problem that is faced in microreactor technology. This study will try to obtain flow distribution among the best that are found in literature: a flow non-uniformity of less than 10 percent. This research also aims to number up to 8 reactor channels and this numbering-up will be done via two types of reactors: a multi-channel micromixer and flexible capillary microreactors.
More importantly, also a model reaction (photocatalytic aerobic oxidation of thiophenol to phenyl disulfide), as showed in Figure 4, will be applied. By applying a reaction the process of numbering-up gets more complicated to due to the fact that reactions will affect the hydrodynamics and pressure drops significantly. The goal is to obtain the same reaction kinetics and performance in the numbered up microreactors compared to a single (capillary) microreactor. For the capillary microreactors it should be noted that this reactor concept allows the throughput and yield to be measured per reactor channel thus making it possible to map the distribution and differences among the different channels in the numbering-up systems.
Furthermore, there is no available literature about the internal numbering-up for photochemical processes, in which the integration of parallel channels or capillaries with different light sources is carefully constructed. Light sources should be numbered-up together with the capillaries as the photon flux should remain constant in order to keep the same photochemical performance in each capillary. In this study the reactor will be designed in such a way that output (e.g. yield, throughput) can be determined for each channel individually.

Chapter 3

Experimental section

Chapter 3 states the chemicals that were used and the analysis equipment used to perform this research. An overview of all of the reactor configurations is shown. Furthermore, the reaction procedures are explained.

3.1 Used chemicals

Thiophenol, α-α-α-Trifluorotoluene, Ethyl acetate, N,N,'N,'N-tetramethylethylenediamine and Eosin Y are obtained from Sigma-Aldrich. NH_4CL, n-Hexane and ethanol are obtained from VWR. Methylene blue is obtained from Merck.

3.2 Analysis equipment

GC-FID: Varian 430-GC Gas Chromatograph.

3.3 Reactor setups

This section shows all of the reactor configurations used to conduct this research. The setups of the micromixer and the multi-capillary microreactors are represented. It should be noted that the capillary microreactor is not expensive: the total price is even below € 100,- (e.g. the price of the capillary itself is only € 13,- per meter). Aside of the low costs it is very easy to assemble the reactor, this assembly process will take approximately 30 minutes without any experience. Subsequently, this reactor technology can be implemented very quickly in each laboratory. Su et al. already described the procedure to make the capillary reactors as follows: "In order to closely integrate the light sources and the capillary microreactor, commercial light stripes with small scale LEDs (Paulmann Lighting GmbH) were used in the experiments. A transparent capillary made of high purity perfluoroalkoxy alkane (PFA from IDEX Health and Science, transmission of 91–96% for visible light with wavelength of 400–700 nm; ID: 750 lm; length: 2.15 m; volume: 1 mL) was coiled around the outer wall of a 20 mL plastic syringe, which was coated with aluminum foil to refract the photons toward the reactor. A LED stripe was coiled around the inner wall of a larger plastic syringe (100 mL), with all LED pillars (3 mm width and 2.5 mm height for each pillar) facing toward the central axis of this syringe. The syringe coiled with the capillary was fixed inside a larger diameter syringe. Consequently, a narrow gap between the LED pillars and the coiled capillary was ensured. Furthermore, pressurized air was supplied through the nozzle of the larger syringe in order to keep the whole system at room temperature (23±1°C), which could be detected by a thermometer."[12] The mass flow controller used was obtained from Bronckhorst.

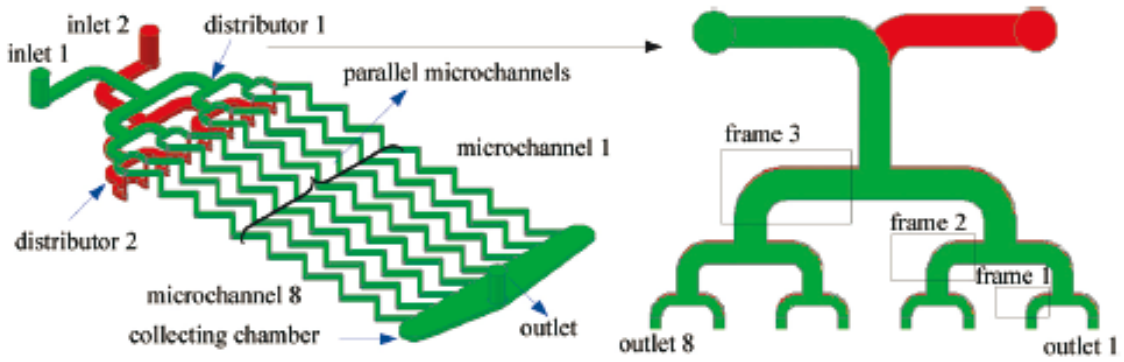

Figure 7: Schematic representation of the multichannel micromixer[17]

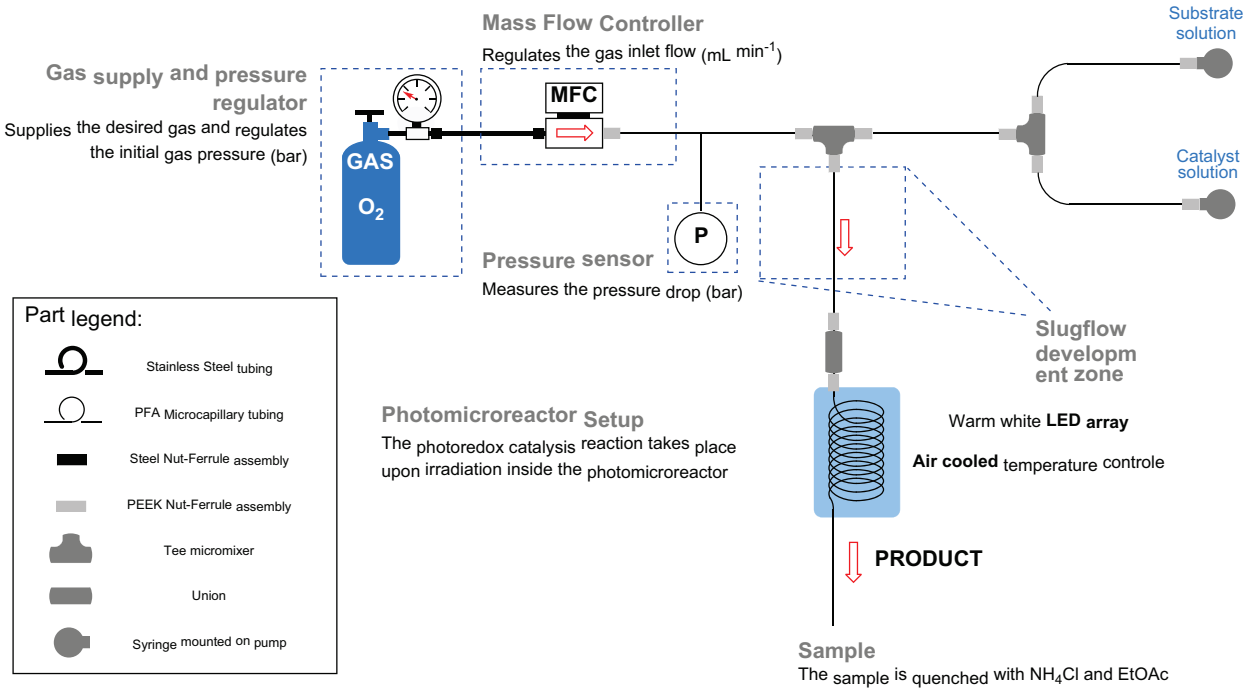

Figure 8: Schematic overview of the single capillary reactor system

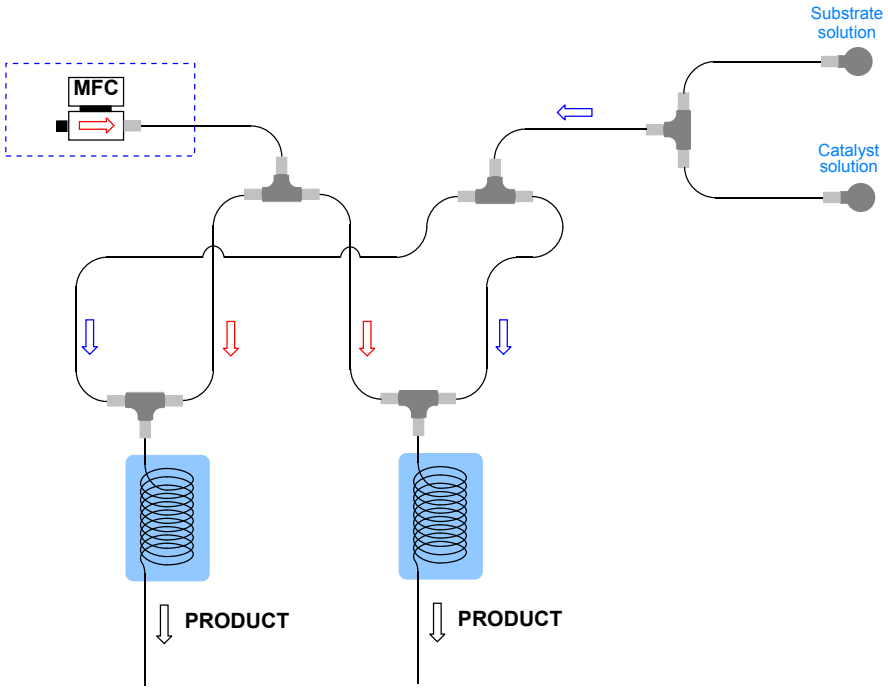

Figure 9: Schematic overview of the two capillary system with gas and liquid splitting individually

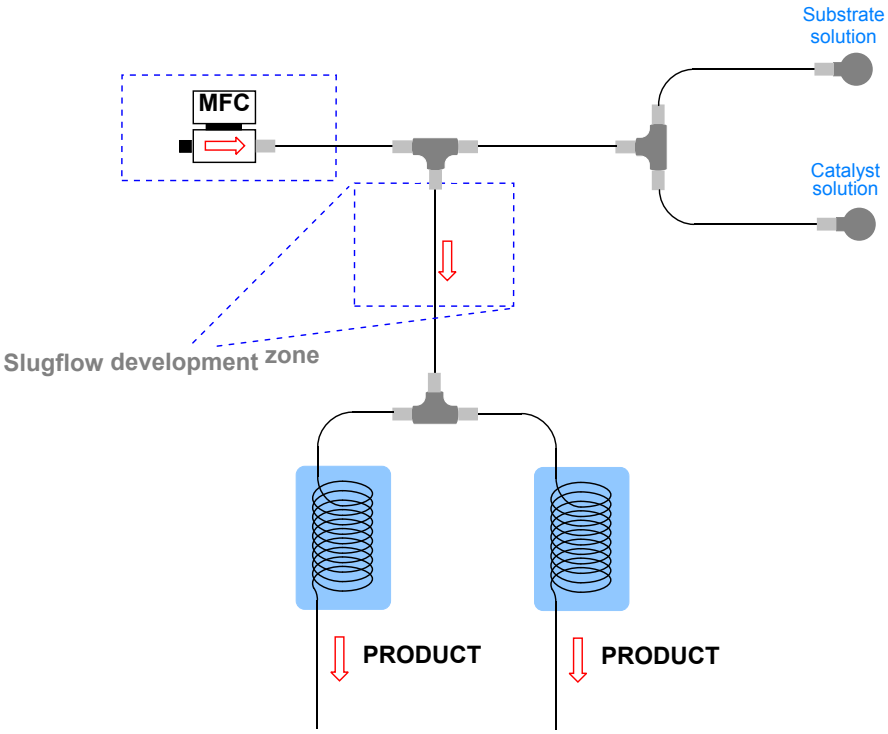

Figure 10: Schematic overview of the single coiled two capillary system

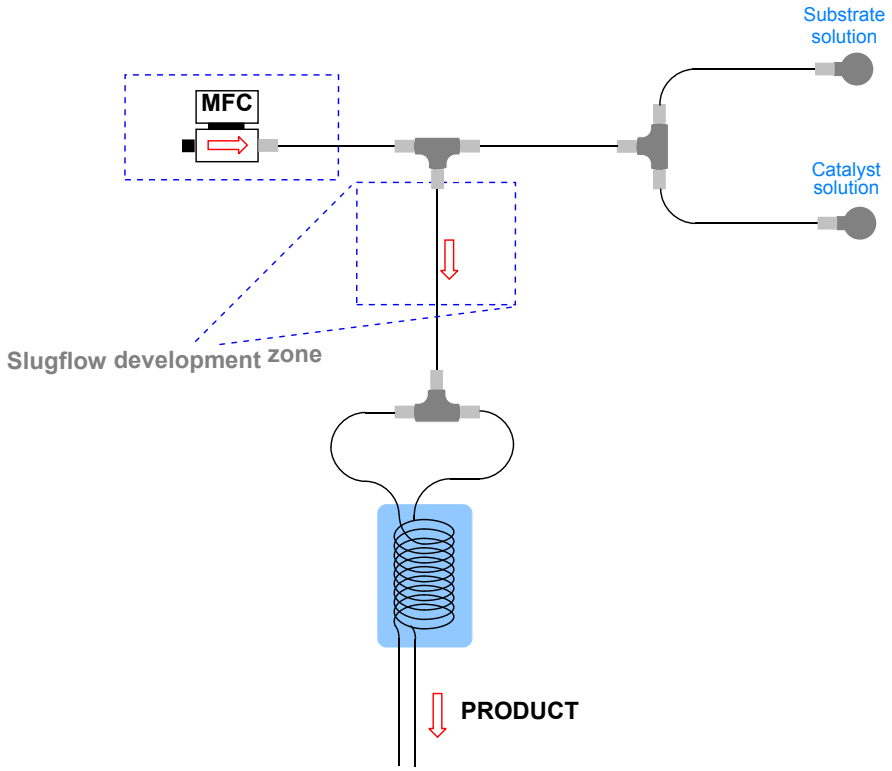

Figure 11: Schematic overview of the double coiled two capillary system

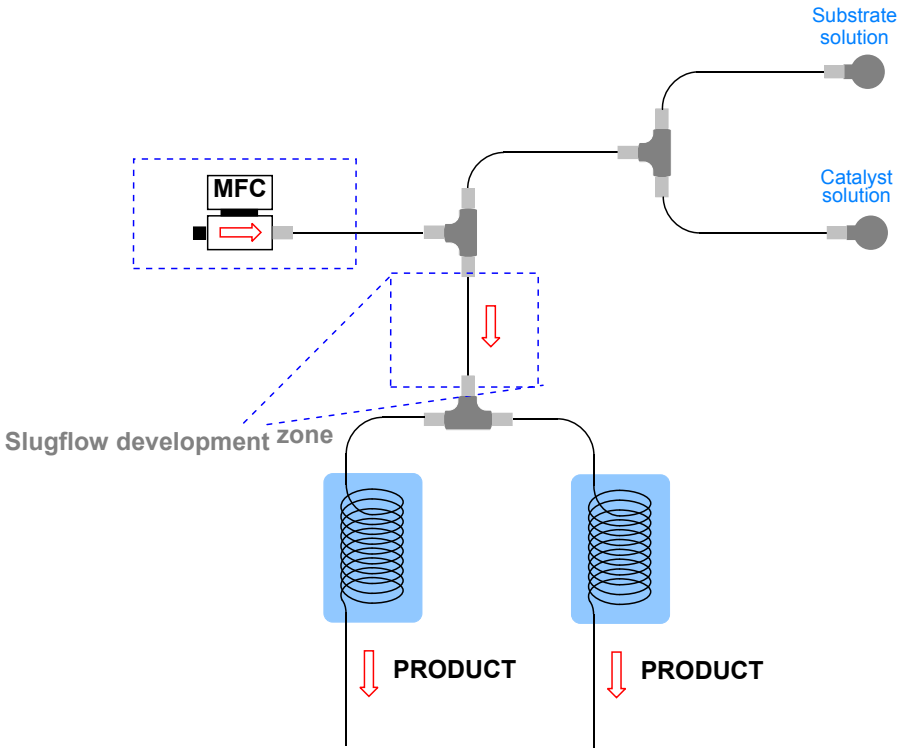

Figure 12: Schematic overview of the single coiled two capillary system with Asymmetric T-mixer orientation

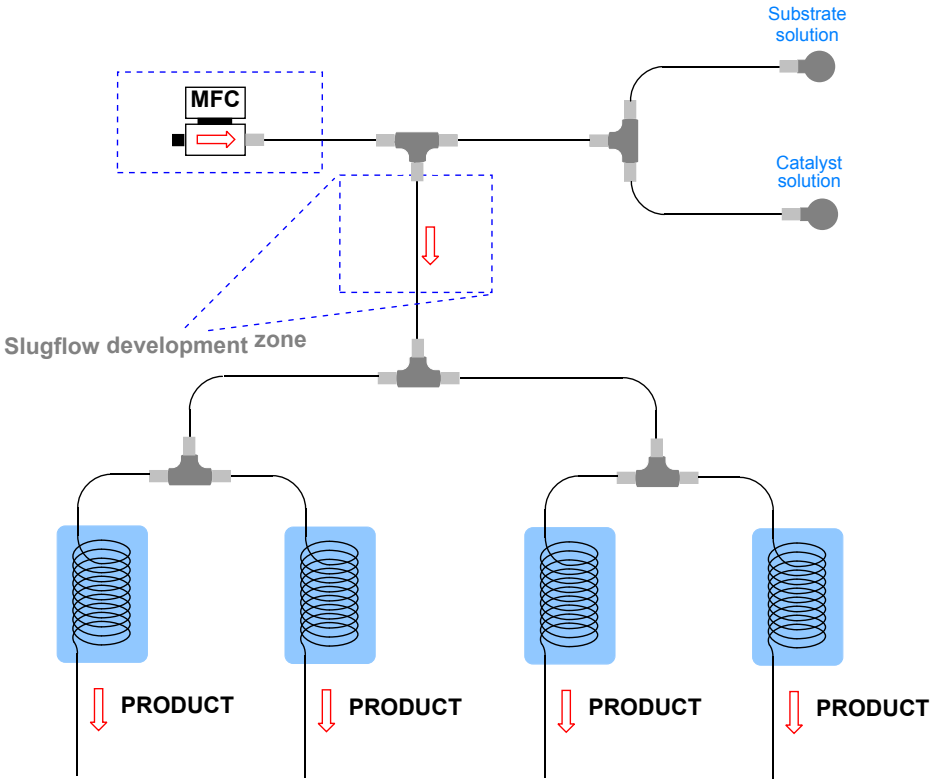

Figure 13: Schematic overview of the single coiled four capillary reactor system

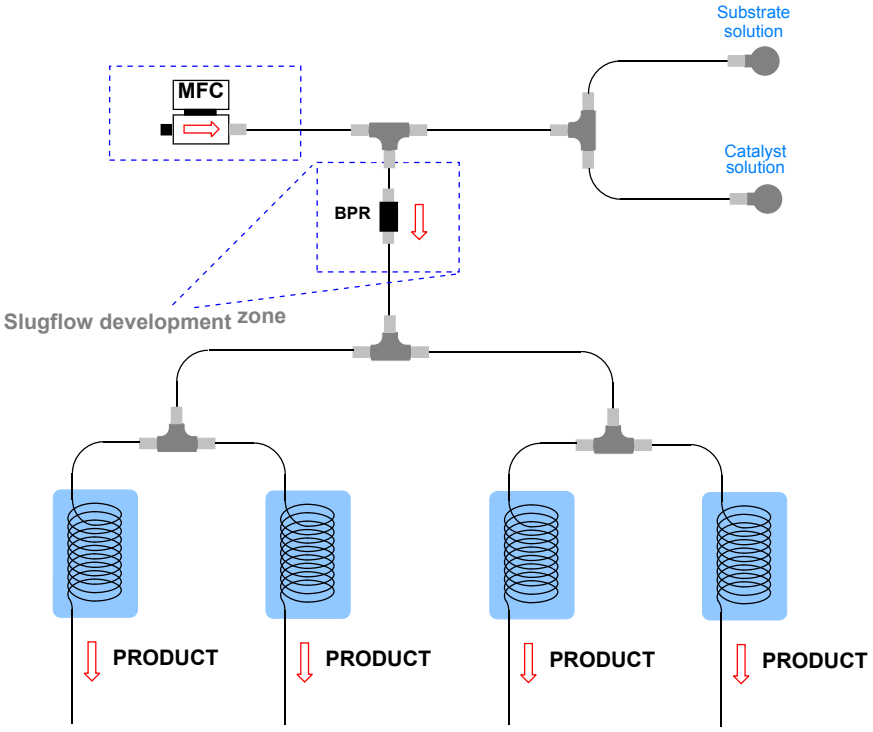

Figure 14: Schematic overview of the single coiled four capillary reactor system with back pressure regulator (BPR)

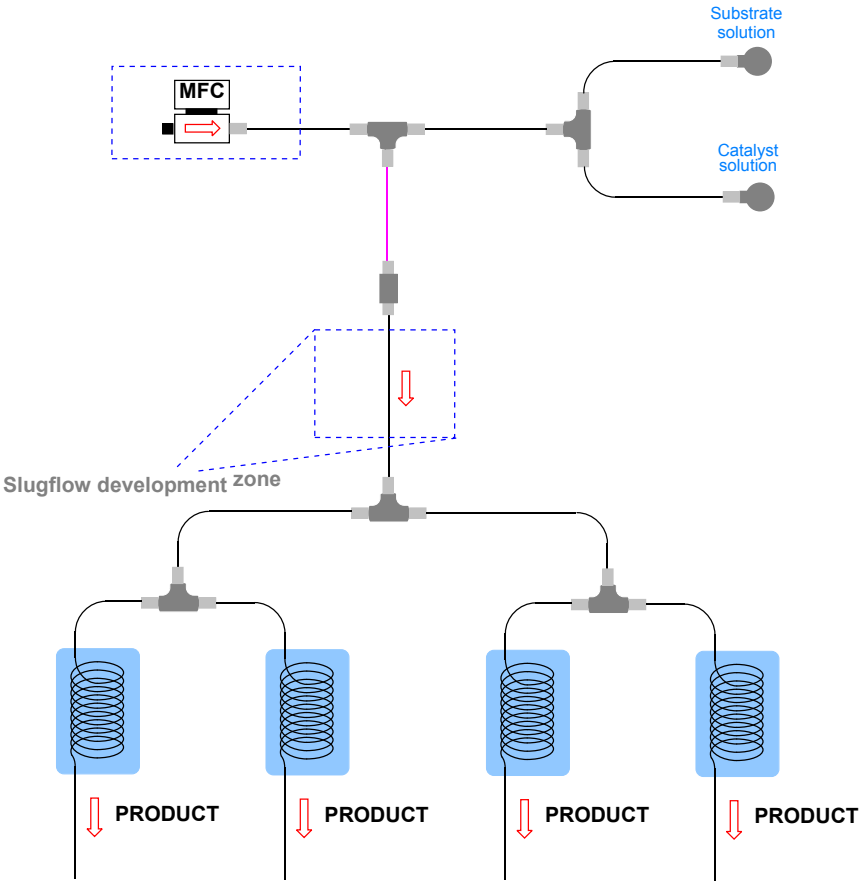

Figure 15: Schematic overview of the single coiled four capillary with smaller tubing for increased pressure drop

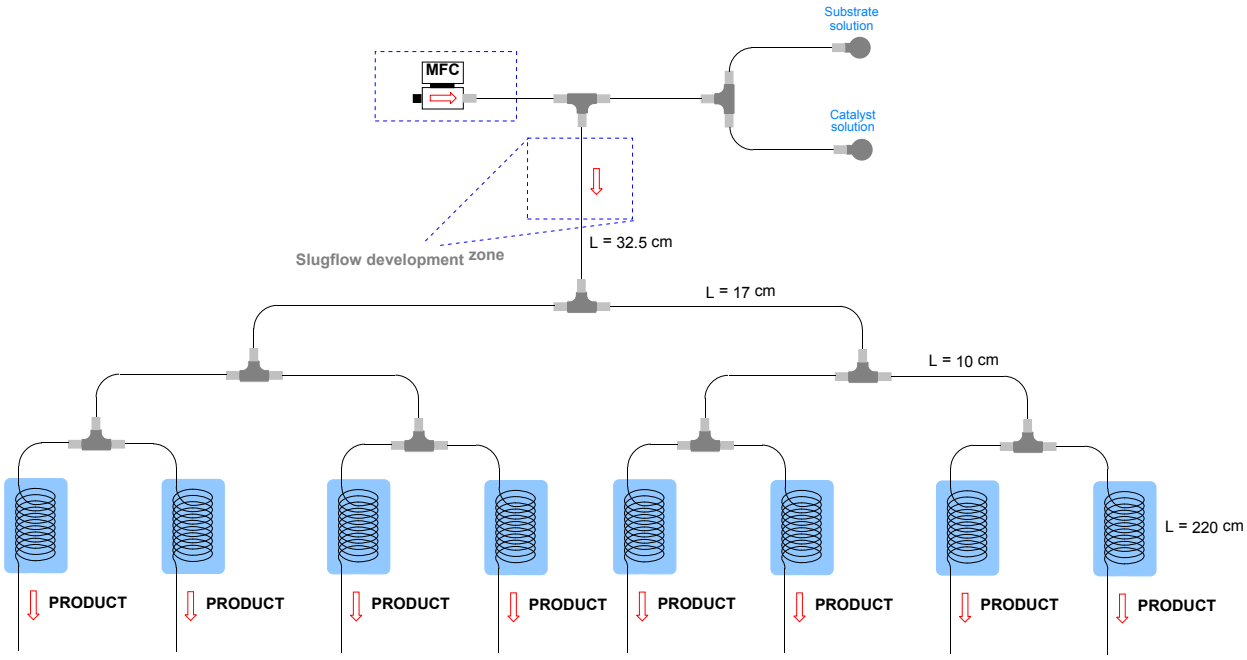

Figure 16: Schematic overview of the single coiled eight capillary reactor system

3.4 Reaction procedure

3.4.1 Multi-channel micromixer experiments

Liquid-liquid slug flow experiments
Methylene blue is dissolved in demineralized water in order to create a blue colored liquid phase. In order to conduct the experiments in the multi-channel micromixer one syringe of 20 mL is filled with the blue colored water phase, and another 20 mL syringe is filled with transparent heptane. The flow rates of immiscible liquid-liquid two phases are controlled by a syringe pump (Fusion 200 classic obtained from Chemyx). Both liquids are collected at the outlet of the micromixer.

Gas-liquid slug flow experiments
The previous mentioned blue colored water phase is placed in a 20 mL syringe and oxygen is introduced into the multi-channel micromixer via a MFC with a gas-liquid flow ratio of 3:1. The gas and liquid are mixed at the T-junctions of the channels in the micromixer as can be seen in Figure 7.

3.4.2 Capillary reactor experiments

A substrate solution containing 0.50 M thiophenol, and 0.25 M trifluorotoluene as an internal standard, in ethanol is made. To protect the substrate solution from light, it is wrapped in alumina foil. Also, a catalyst solution is prepared: 1 mol% Eosin Y and 1 molar equivalent TMEDA based on the substrate is dissolved in ethanol.

A syringe is filled with the substrate solution, while another similar syringe is filled with the catalyst solution. The two solutions are mixed via a T-mixer and hereafter, also via another T-mixer, contacted with oxygen gas resulting in slug flow. This segmented flow should have enough time to develop fully before entering the reactor. The reaction of the mixture is activated in the reactor by visible light from a 1.5 m LED light source (4.8 W, 420 lm, daylight obtained from Paulmann Lighting GmbH)). An overview of this process can be seen in chapter 3.3. At the end of the reactor a sample is taken and the reaction is quenched with a saturated NH_4Cl solution and EtOAc. The sample is purified over a mini silica column and analyzed with GC-FID.

Chapter 4

Results and discussion

In this chapter a theoretical residence time, as showed in Equation (6), is used to compute multiple figures. This theoretical residence time, based on reaction stoichiometry, takes the oxygen consumption and pressure drop in capillaries under reaction conditions into account.

$$\begin{aligned}\tau &= \frac{V_c}{Q_G + Q_L} = \frac{V_c}{\frac{Q_{G,in} + Q_{G,out}}{2} \times \frac{P_{out}}{(P_{in} + P_{out})/2} + Q_L} \\ &= \frac{V_c}{\frac{Q_{G,in} + (Q_{G,in} - 0.25 Q_L C_{sub,0} RTY / P_{out})}{2} \times \frac{P_{out}}{(P_{in} + P_{out})/2} + Q_L}\end{aligned} \tag{6}$$

The average yield (Y) is calculated based on a weight average (yield) calculation, represented in equations (7), (8) and (9), meaning that the measured yield and weight fraction for each outlet respectively are taken into account.

$$Y = w_1 Y_1 + w_2 Y_2 + \ldots + w_k Y_k \tag{7}$$

With $Y_{k,i}$ being a dataset of at least two data points, $i \geq 2$, and two outlets, $k \geq 2$.

$$Y_k = \frac{Y_{k,i} + Y_{k,i+1} + \ldots + Y_{k,n}}{n} \tag{8}$$

$$w_k = \frac{W_{k,i} + W_{k,i+1} + \ldots + W_{k,n}}{n} \tag{9}$$

It is assumed that w_k and Y_k are independent variables. Then the standard deviation of the yield can be calculated according to Equations (10) and (11). This results in a confidence interval (CI) of the average yield as can be seen in Equation (12).

$$\begin{aligned} VAR(Y) &= VAR(w_1Y_1 + w_2Y_2 + \ldots + w_kY_k) = VAR(w_1Y_1) + VAR(w_2Y_2) + \ldots + VAR(w_kY_k) \\ &= E(w_1^2)E(Y_1^2) - [E(w_1)]^2[E(Y_1)]^2 + E(w_2^2)E(Y_2^2) - [E(w_2)]^2[E(Y_2)]^2 \\ &+ \ldots + E(w_k^2)E(Y_k^2) - [E(w_k)]^2[E(Y_k)]^2 \end{aligned} \quad (10)$$

$$\sigma_Y = \sqrt{VAR(Y)} \quad (11)$$

$$CI = Y \pm \sigma_Y \quad (12)$$

The deviation on the flow rates (hydrodynamics) among each capillary are based on the weight output and have an analogous derivation, as can be seen in Equation (13) to (15).

$$VAR(w) = VAR(w_1 + w_2 + \ldots + w_n) \quad (13)$$

$$\sigma_w = \sqrt{VAR(w)} \quad (14)$$

$$CI = w + \sigma_w \quad (15)$$

4.1 Multi-channel micromixer

In chapter 4.1 the distribution performance of the multichannel micromixer, as represented in Figure 7, is tested. To quantify this performance a hydrodynamic study is done. Both a liquid-liquid and a gas-liquid system are tested. As the model reaction was previously done in the solvent ethanol, it would be convenient to also apply this system to the multichannel micromixer for comparison reasons. The multichannel micromixer is made of two PMMA plates, which form a chip reactor. However, the PMMA is dissolvable in ethanol. Therefore, a heptane-water and an oxygen-water system are used as liquid-liquid and gas-liquid system, respectively. The micromixer consists of eight channels with both a width and depth of 500 μm and an overall length of 53 mm[17].

4.1.1 Liquid-liquid system

Different flow rates are tested in order to obtain equal distribution, varying from 0.5 ml/min to 20 ml/min for both phases. As can be seen in Figure 17, at the lower throughputs no equal distribution is obtained. Only for very high throughputs, circa 20 ml/min, the distribution amongst the channels is equal. This latter throughput is translated to a superficial velocity of .33

m/s and a residence time of 0.16 seconds, while previous research shows that a residence time in the order of minutes is necessary[11]. It could be that the zigzag structure of the channels, which is not symmetric in orientation, disturbs the equality of the flows due to a pressure drop difference over the channels.

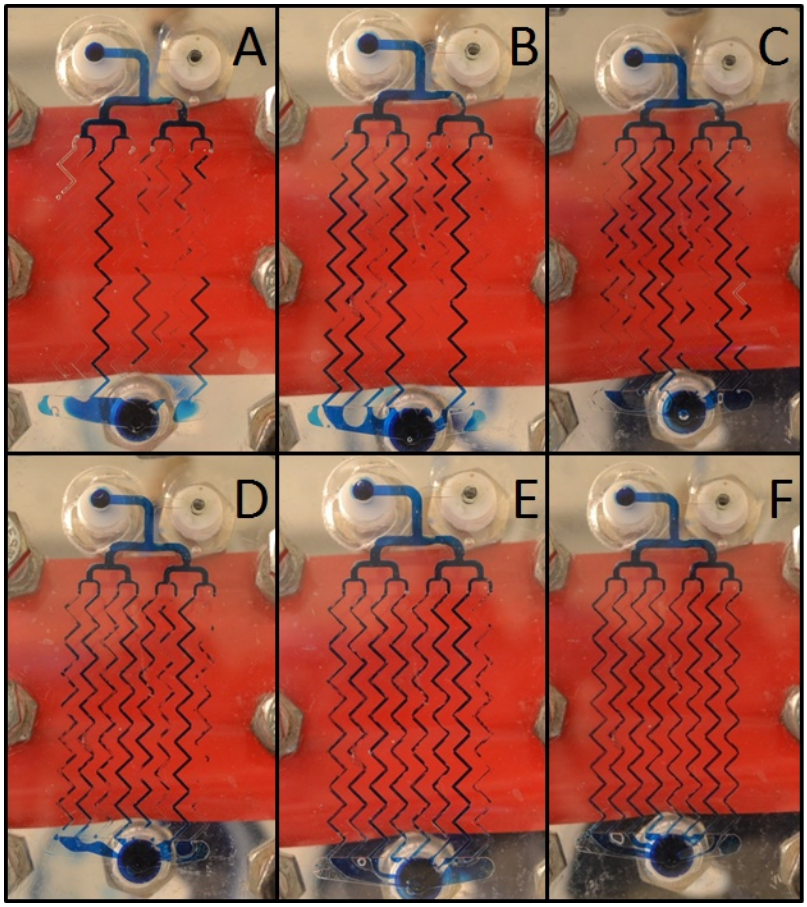

Figure 17: Photographic view of the heptane-water system in the multichannel micromixer for different heptane and water throughputs: 0.5 ml/min (A), 1 ml/min (B), 2 ml/min (C), 5 ml/min (D), 10 ml/min (E), 20 ml/min

$$Ca = \frac{\mu v}{\gamma} \tag{16}$$

For these experiments capillary numbers, as stated in Equation (16), vary from $6.6 \cdot 10^{-5}$ up to $2.6 \cdot 10^{-3}$. As a rule of thumb there can be used that for values of the capillary number higher than 10^{-5} the viscous forces exert the capillary forces, thus meaning that capillary forces have significant influence for the lower throughputs. To overcome possible limitations in the distribution due to surface tension between the liquid phases, the experiments are repeated with the surfactant Span 80. Different concentrations of surfactant are used: 0.5 wt%, 1 wt% and 2 wt%.

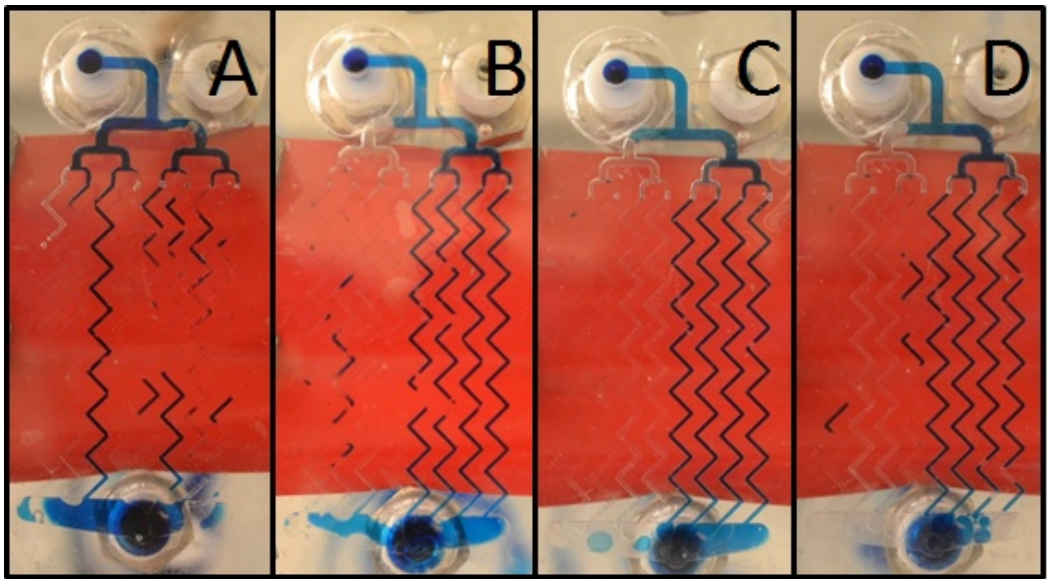

Figure 18: Photographic view of the heptane-water system in the multichannel micromixer for a heptane and water throughput of 0.5 ml/min and different surfactant concentrations: no surfactant used (A), 0.5 wt% Span 80 (B), 1 wt% Span 80 (C), 2 wt% Span 80 (D)

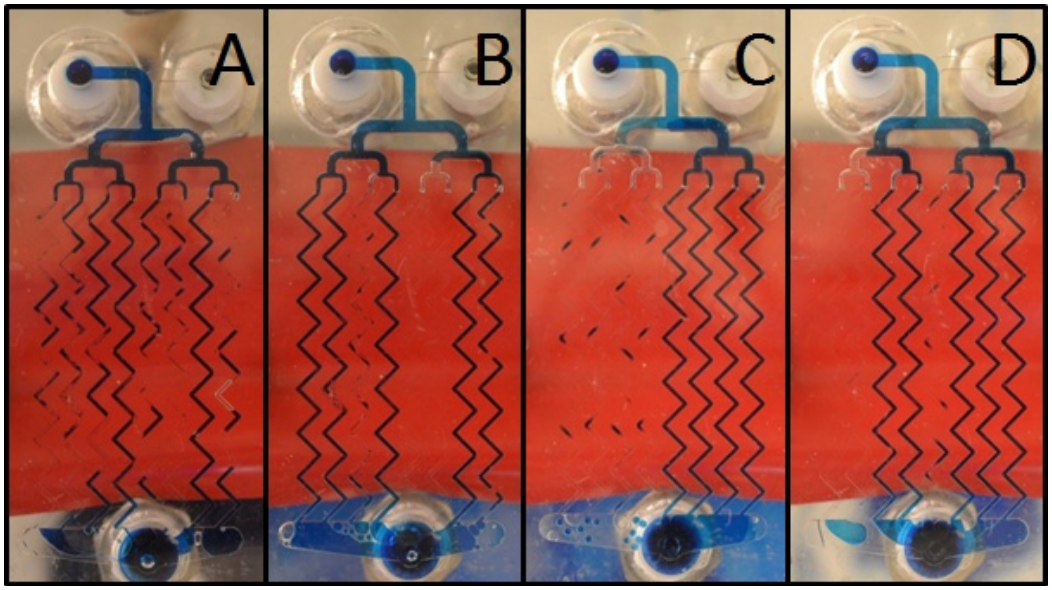

Figure 19: Photographic view of the heptane-water system in the multichannel micromixer for a heptane and water throughput of 2 ml/min and different surfactant concentrations: no surfactant used (A), 0.5 wt% Span 80 (B), 1 wt% Span 80 (C), 2 wt% Span 80 (D)

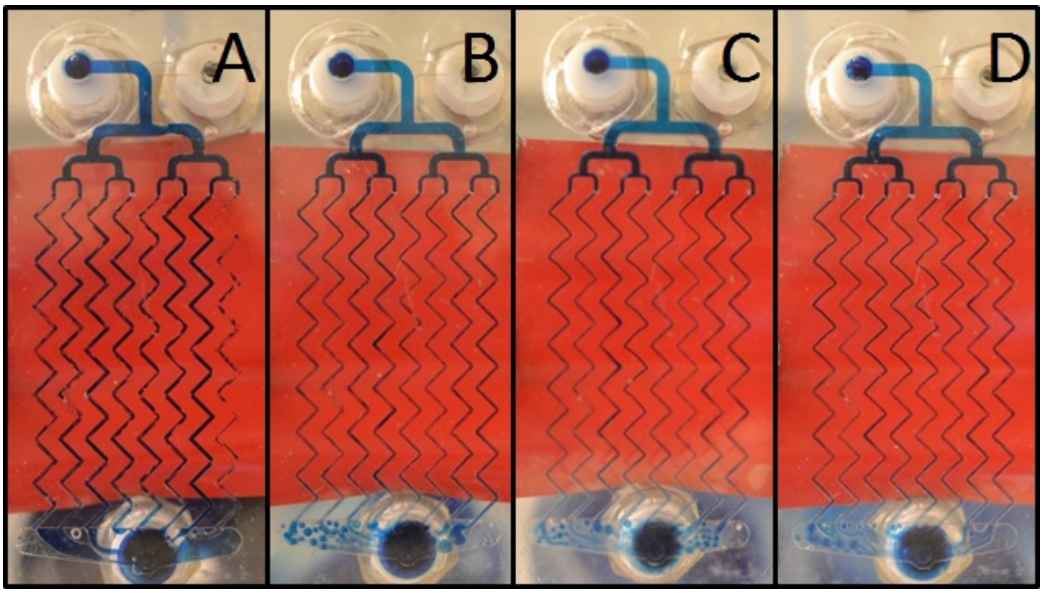

Figure 20: Photographic view of the heptane-water system in the multichannel micromixer for a heptane and water throughput of 10 ml/min and different surfactant concentrations: no surfactant used (A), 0.5 wt% Span 80 (B), 1 wt% Span 80 (C), 2 wt% Span 80 (D)

Figure 18, Figure 19 and Figure 20 show that addition of surfactant only has a small positive contribution to the distribution. For instance, when Figure 17 and Figure 20 are compared it can be observed that with the use of surfactant equal distribution is obtained at heptane and water throughputs of 10 ml/min compared to 20 ml/min with the case when no surfactant is used. In Figure 18 and Figure 19 three types of microchannels can be distinguished: channels containing the blue colored water phase, the transparent heptane phase and channels containing both phases. These figures show that the use of surfactant has little influence on the distribution at low flow rates, with throughputs of 0.5 ml/min and 2 ml/min, respectively. The surfactant; however, stabilizes droplets of liquid collected at the outlet of the channels, as can be seen in the collector part. There can be concluded that the capillary force dominates the distribution at low flow rates and the distribution mainly depends on the viscous force at high superficial velocity.

4.1.2 Gas-liquid system

As the model reaction is a gas-liquid system, also research on the distribution of an oxygen-water system is conducted: a volumetric flow ratio of oxygen to water of 3:1 is used. As the reaction can probably only reach significant conversion in low residence times, liquid throughputs of 0.5 ml/min, 1 ml/min and 2 ml/min are tested. The results can be seen in Figure 21. It is shown that equal distribution is also not obtained within the gas-liquid system. However, there can also be seen that the distribution of the gas-liquid system is even inferior compared to the liquid-liquid system showed previously (see Figure 17B and Figure 21B). This is attributed to larger interfacial tense between gas-liquid two phases than that for liquid-liquid two phases. That is, the capillary force in gas-liquid two-phase systems occupies a more important role on the fluid distribution in multi-channel micromixers. As the residence time is very short and only unequal distribution could be obtained, there is concluded that this device is unsuitable for application of the model reaction.

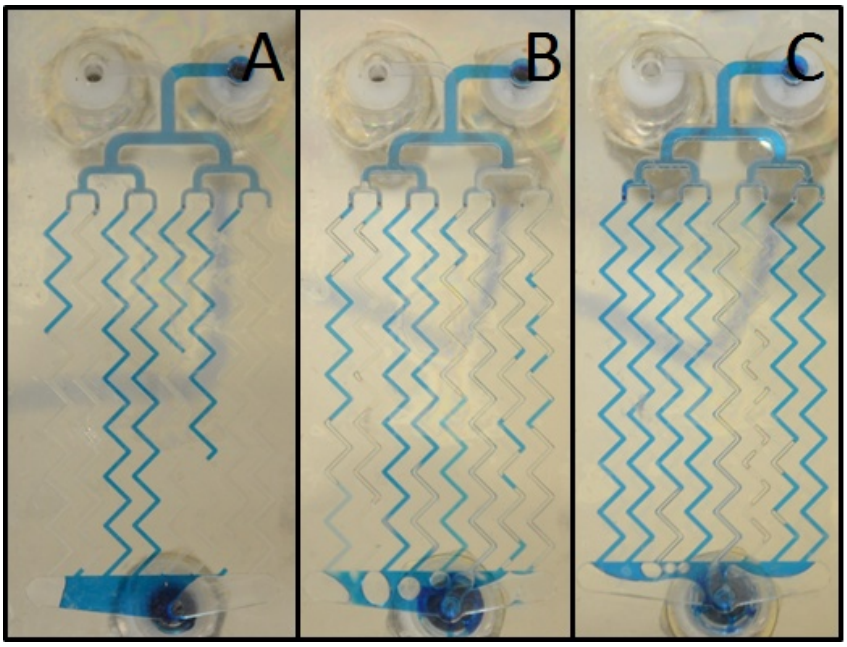

Figure 21: Photographic view of the oxygen-water system in the multichannel micromixer for different gas and liquid throughputs: 0.5 ml liquid/min (A), 1 ml liquid/min (B), 2 ml liquid/min (C)

4.2 Capillary reactor

4.2.1 Hydrodynamics

In this chapter the results of the hydrodynamic study will be presented. Firstly, the numbering-up systems with excellent distribution performance are discussed. Subsequently, alternative tested systems will be evaluated for the two-capillary systems and for the four-capillary systems.

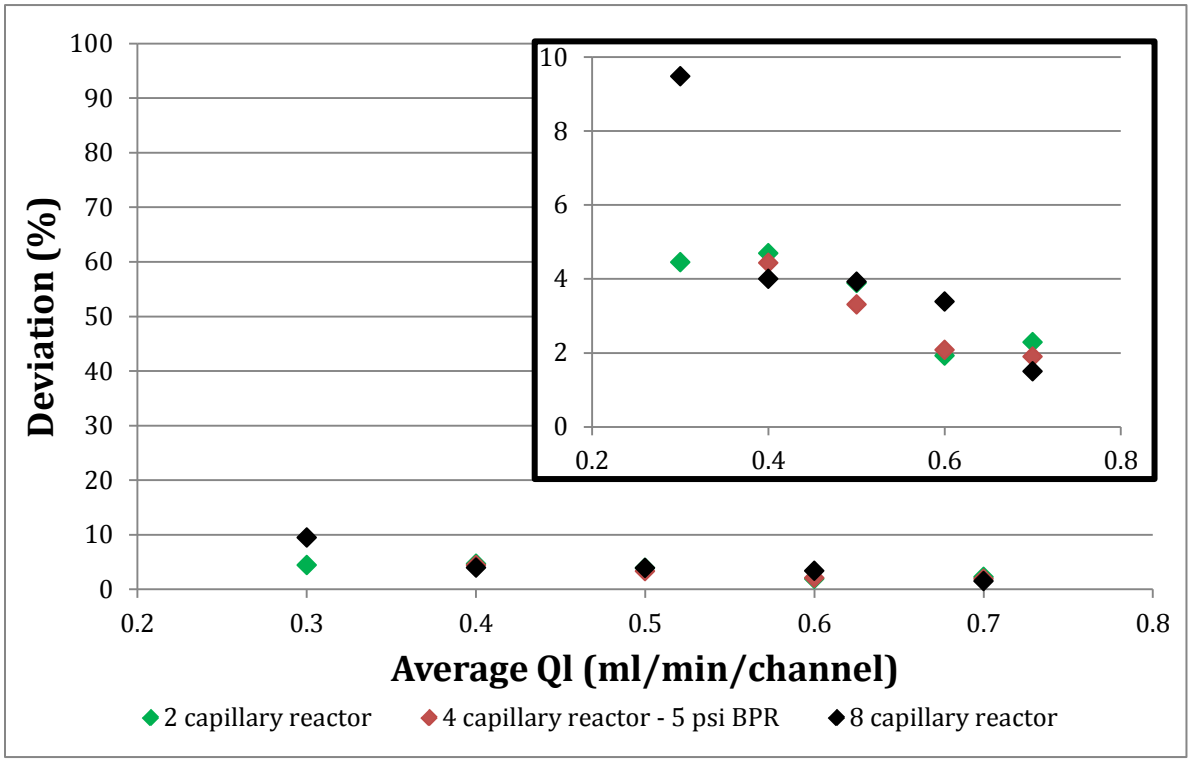

Figure 22: Hydrodynamics; performance of 2 capillary, 4 capillary with 5 psi BPR and 8 capillary system

In Figure 22 the quality of the best performing systems is shown on a 100 percent scale as well as on a zoomed in scale. The four-capillary system performed best when a pressure regulator was used as a resistance (Figure 14) to increase pressure drop in the distributor part of the system as is explained in Equation (5). The setups for the two- and eight-capillary systems, as described in Figure 22, can be seen in Figure 10 and Figure 16, respectively. Figure 22 also shows that the quality for scale-up is very good for flow rates of 0.4 ml/min/channel and higher as the data points are (almost) overlapping. For the low flow rate of 0.3 ml/min/channel instabilities of the flow rate already existed in the single capillary system. In the multi-capillary systems it can be seen that the deviation of flow rates among parallel capillaries is significantly higher than for the higher flow rates. These findings indeed accord with the previous results for the multi-channel micromixer. At low flow rates, the interfacial force plays a non-negligible role in the fluid distribution and thus in the numbering-up processes. Meanwhile, low flow rates result in relative small local pressure drop arising from the fluid splitting in T-micromixers,

which is not beneficial for fluid distribution. When the 0.3 ml/min/channel flow rate was tested for the four-capillary system with constriction in the distributor part the flow even stalled in one or multiple channels, so good distribution could not be obtained. Probably the capillary forces have significant contribution compared to the viscous forces at the lowest tested flow rate. Moreover, the constriction also induced a part of flow instability. Therefore, pressure drop, interfacial force and flow stability obviously affect the fluid distribution in this kind of distributors with T-micromixers as splitting units. It should be noted that the flow rate deviation in distribution for the stable flow rates is less than 5 percent, where, as mentioned before, deviations of 10 percent are found in literature[30].

Two-capillary system

For the scale-up multiple alternatives for the setup of Figure 10 are tested. It has been tried to first split-up the gas and liquid flows individually with two different T-micromixers and then combine gas and liquid flows as is depicted in Figure 9. Moreover, studies on bubble break-up are already done[25,27,28,32] and it shows that the orientation of a splitting unit can have great influence on bubble break-up and, therefore, distribution. In order to quantify this influence a setup with the T-mixer (used as splitting unit) orientated asymmetric is tested, as can be seen in Figure 12.

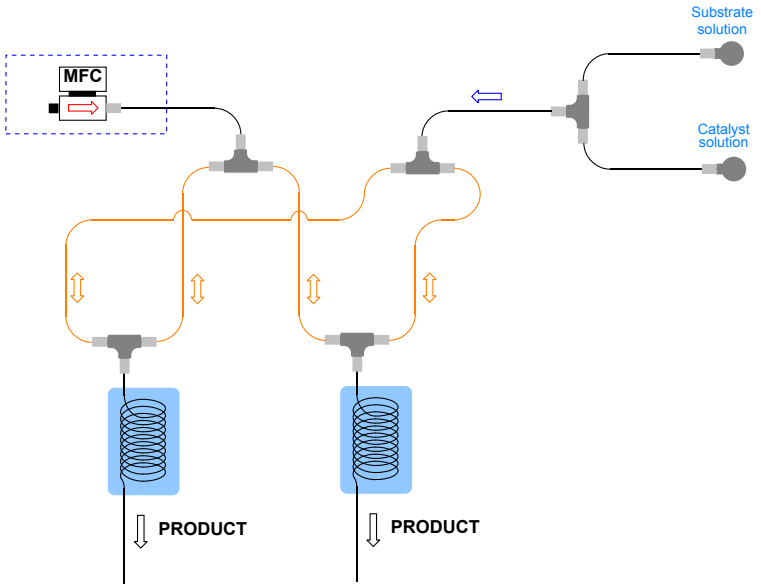

Figure 23: Circular flow in two capillary system with gas and liquid flows split up individually

The system where gas and liquid stream are split up individually (Figure 9) could not establish equal distribution. Circular flow in the system was even obtained, as can be seen in the orange colored part of Figure 23. After enough pressure was build up due to the accumulation of fluid, gas and liquid would shoot through one of the reactors randomly. Apparently, the pressure drop in the reactors is high enough to establish the circular flow. Therefore, this strategy with respectively splitting gas and liquid two phases cannot work well in the numbering-up of capillary microreactors.

A comparison of a symmetric and asymmetric orientation of the splitting unit is made in Figure 24. There can be seen that the symmetric configuration gives a more stable flow distribution and it also allows the flow to split up at a flow rate of 0.3 ml/min, whereas good splitting cannot be achieved with the asymmetric orientation.

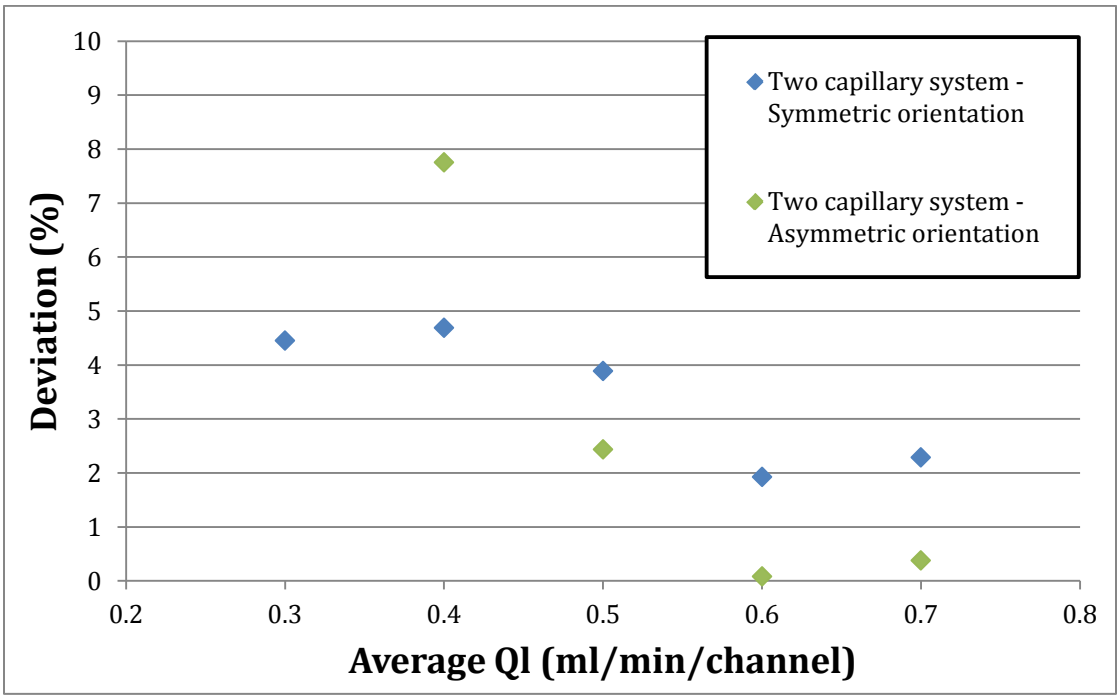

Figure 24: Comparison of two capillary system with symmetric and asymmetric T-mixer configuration

Four-capillary system

As the principle of pressure drop adjustment, as explained in the theory and stated in Equation (5), can have significant influence on the flow distribution this phenomenon is researched. Multiple increased resistances are tested and compared with the case of no increased resistance (d=750µm). These results are shown in Figure 25 on a 100 percent scale and a zoomed scale. It can be seen that the BPRs do not contribute to a better distribution at the lowest flow rate, because there is observed that in one or multiple capillaries the flow stalls. Furthermore, it can be seen that the systems with the BPRs as resistances show similar results in split-up quality, even though the extra applied pressure drop is different in the two cases presented. It should be noted that the BPRs are designed for homogeneous liquid systems, but appeared to be working for heterogeneous gas-liquid systems as well. The utilization of BPRs results in better fluid distribution for the four highest flow rates, because of the pressure drop theory stated in Equation (5). How the pressure drop is build up is depicted in Figure 27, which shows that the pressure drop in the distributor part is significantly higher than in the reactor part. Also, a setup where a piece of small diameter (d=250µm) tubing is added to the slug development zone is tested, which is shown in Figure 15 where the purple line indicates the smaller diameter tubing. Taking the increased pressure drop into account, as is depicted in Figure 26, it seems logical that this case results in a distribution deviation between the cases where the BPRs are used and the case where no increased pressure drop is used. This is as expected because the pressure drop

value is also between these cases. However, when longer capillaries of 250 µm diameter are tested (e.g. 40 cm or longer instead of 33 cm) the system could not cope with the pressure and the pumps stalled. In conclusion a smaller capillary and especially BPRs result in better fluid distribution performance; however, for the lowest flow rate it aggravates the instability of the flow, which leads to a deteriorated flow distribution.

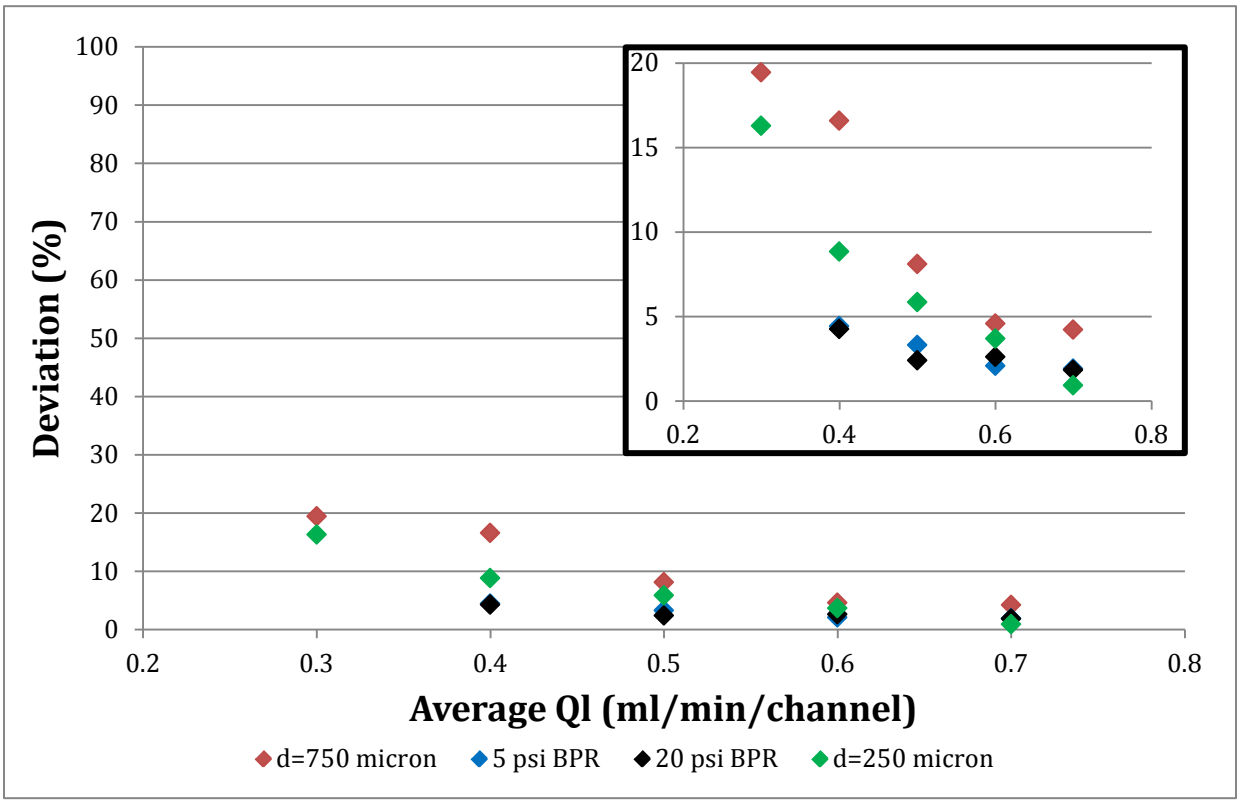

Figure 25: Comparison of different 4 capillary systems

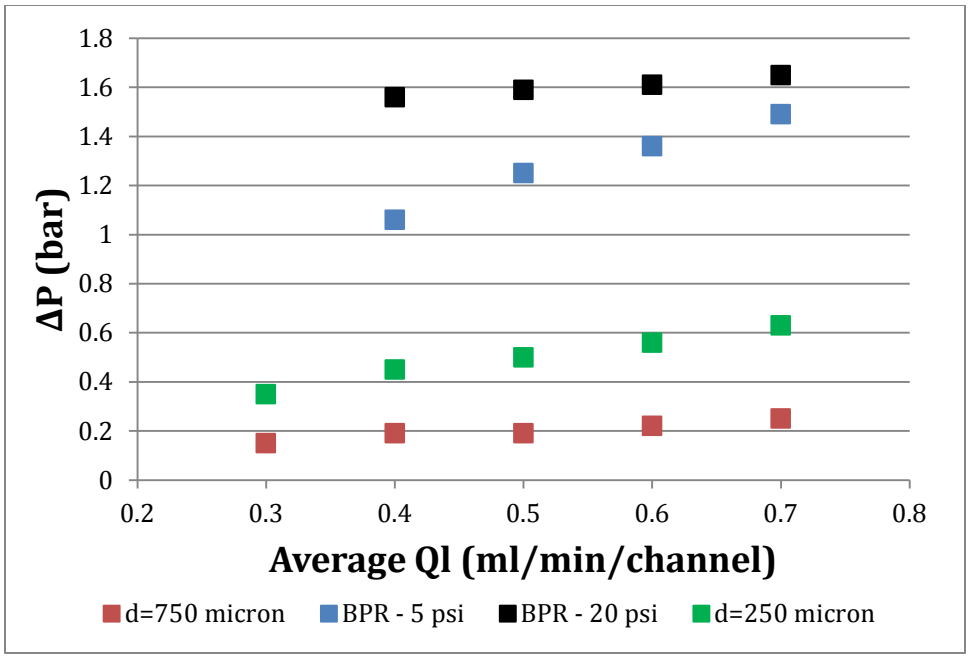

Figure 26: Pressure drop for different 4-capillary system setups

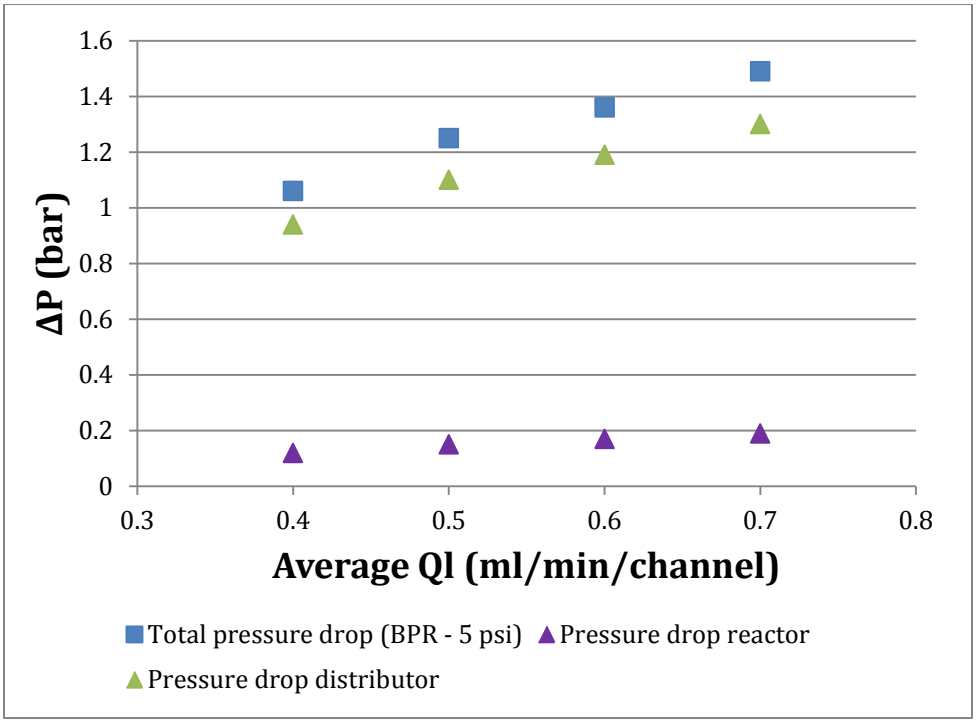

Figure 27: Pressure drop within the 5 psi BPR reactor set-up

4.2.2 Reaction system

Firstly, in order to determine the quality of numbering-up a single capillary reactor is tested as a reference frame. Different light sources are tested to optimize this photocatalytic process as energy transfer via photons is an important factor in photocatalysis. Both spectral overlap between the light source and reaction mixture and quantum efficiency have great influence on the reaction rate. A reactor system similar to Su et al. is used for experimental work. They already have established a mass transfer free zone in the region of residence times lower than 100 seconds and a gas to liquid flow rate of 3:1[12].
The used light sources are quantified in Table 1. Moreover, a comparison of the yield for different light sources can be found in Figure 28. An first order dependency in thiophenol is assumed as stated in Equations (3) and (4). This dependency is verified in Figure 29, where the first order in thiophenol is plotted versus the residence time.

Table 1: Quantification of the light sources used in the single capillary system

Light source	Power (W)	Luminous flux (lm)	Length (cm)	Type of light (according to vendor)
1	3.12	78	97	White
2	3.12	195	97	Warm white
3	2.4	150	100	Neon green
4	4.8	300	150 (100 used)	Warm white
5	4.8	420	150 (100 used)	Daylight

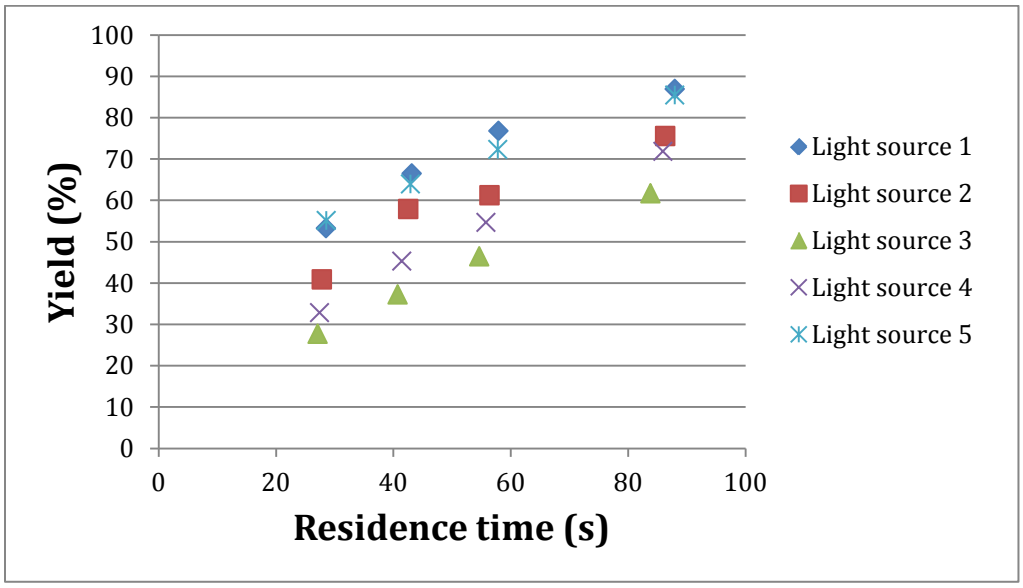

Figure 28: Yield of different light sources in the single capillary reactor

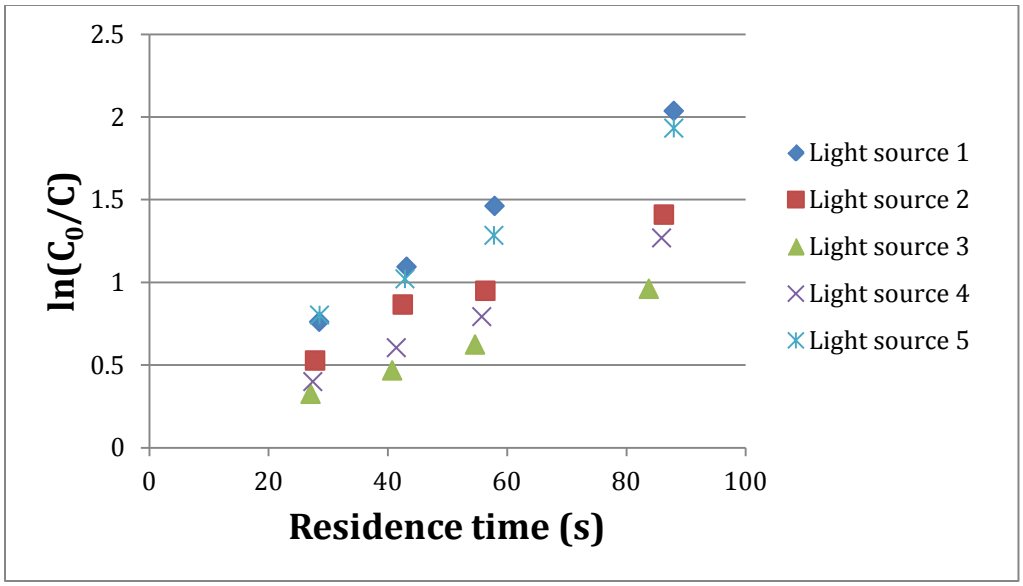

Figure 29: Kinetics of different light sources in the single capillary reactor

From Figure 28 and Figure 29, it can be concluded that the type of light mostly determines the performance of the reaction. There can be clearly seen that light source 1 and 5 perform the best and that the green light source, light source 3, has the lowest reaction rate although green light (490 nm – 570 nm) has the most spectral overlap with the catalyst[12]. However, the intensity of the light is reasonably low compared to the other light sources. Furthermore, experimental results for all light sources further indicate that the assumption of first order kinetics in thiophenol is valid.

Light source 5 is chosen as the most convenient light source to use, because when using the total light source of 150 cm it is able to go to even higher conversions as light source 1. As can be seen in Figure 30, the energy emission is the largest in the 430 to 575 nm region. This show great overlap with the absorption spectrum of Eosin Y, which absorbs the light between 475 and 550 nm as stated in previous work by Su et al[12]. The integration of the emission distribution in Figure 30 gives the total radiant flux. When this value is divided by the total power supply the fraction of emitted light is calculated, as can be seen in Equation (17). Light source 5 converts 0.76 W, thus 15.83% of the energy, into light.

$$\eta_{light} = \frac{\sum_{350}^{750} E_\lambda \lambda}{P_{light\ source}} \tag{17}$$

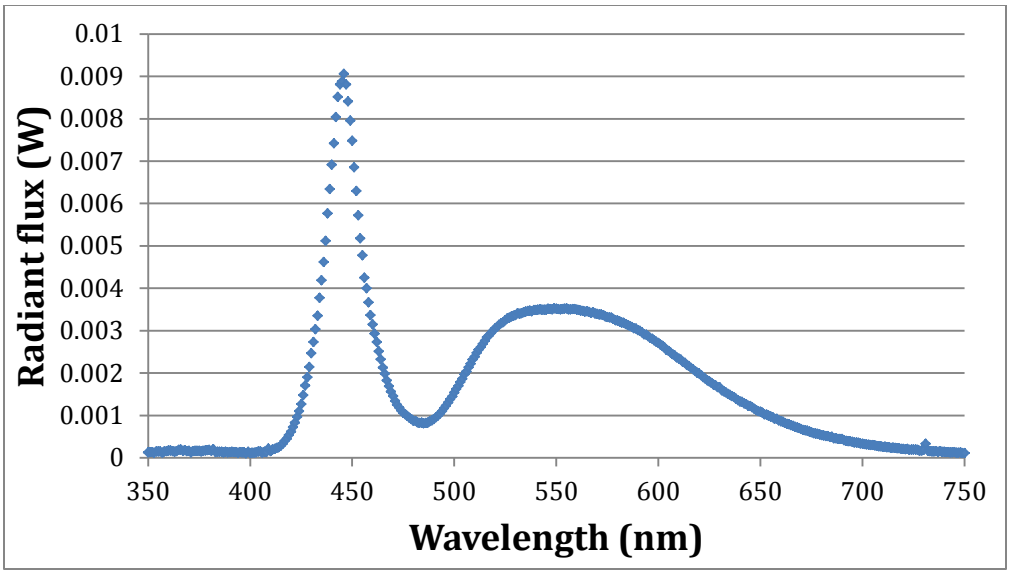

Figure 30: Energy distribution of light source 5

Numbering-up

In this part the reaction performance of the numbered-up reactors will be presented and discussed. The reaction experiments are conducted in the best performing systems concluded from the hydrodynamic study. The single capillary (Figure 8), single coiled two-capillary (Figure 10), single coiled four capillary with a 5 psi BPR (Figure 14) and the single coiled eight capillary system (Figure 16) are tested. The performance is determined based on yield and kinetics.

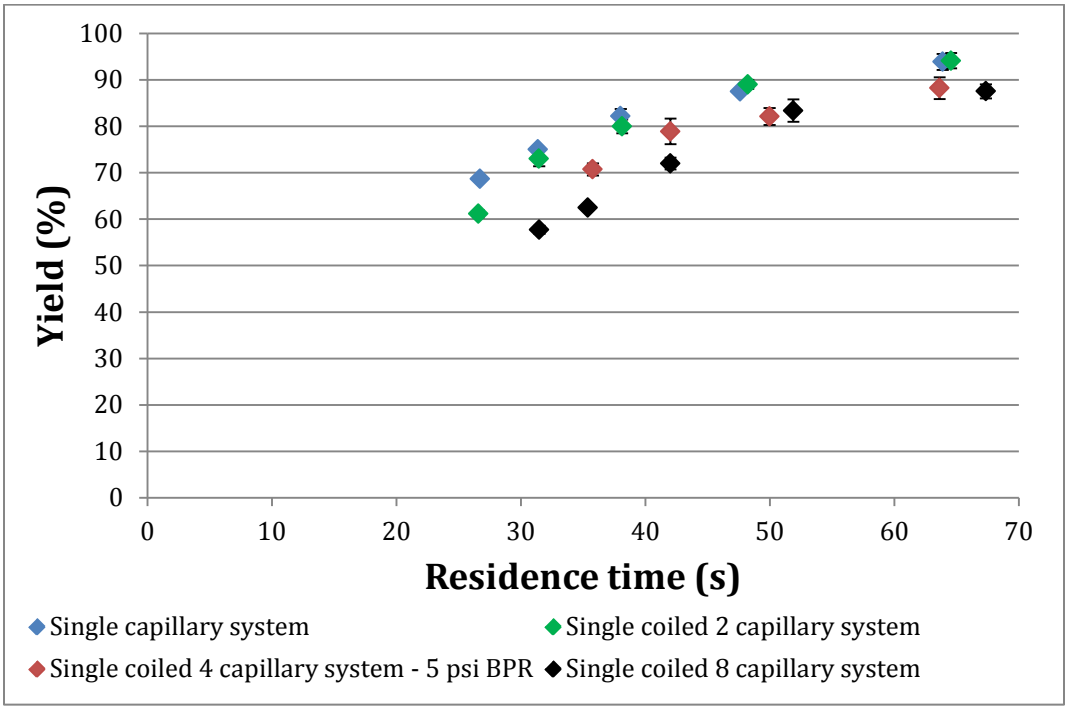

Figure 31: Yield of numbered-up reactors

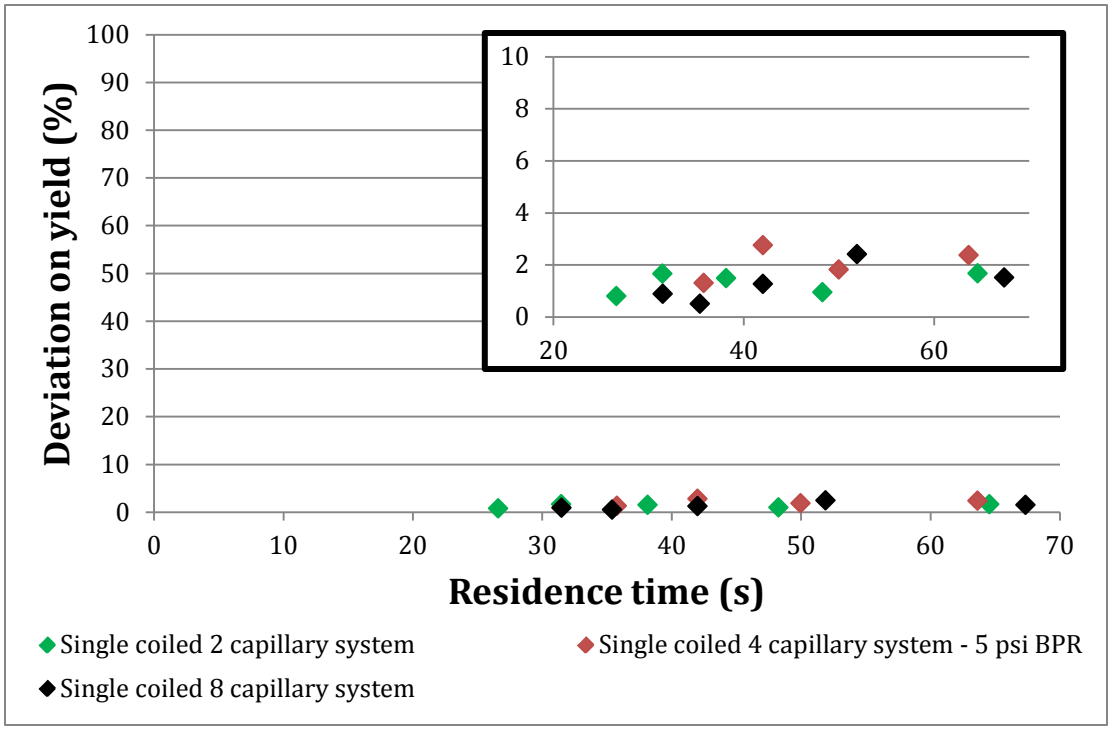

Figure 32: Deviation on yield for numbered-up reactors

The yield of the different reaction systems is represented in Figure 31. This graph shows that the reaction yield slightly decreases with increasing number of capillaries and that the deviation of yield among parallel capillaries on the acquired data is very small, which is shown in the error bars and in Figure 32. As can be seen in Figure 32, the deviation on reaction yield is lower than 5 percent. The decreasing yield is also backed by the first order kinetics, which holds for all the numbered-up reactors, as can be seen in Figure 33. This figure also shows that the single coiled two-capillary reactor performs almost the same as the single capillary reactor. The reaction rate constant only deviates a bit from that in the single capillary system (according to Equation (4)). For four-capillary system, similar reaction performance could be obtained at all average residence times involved. However, for eight-capillary system, the deviation of yield becomes larger as compared with the single capillary system, indicating the necessity of further optimization. Furthermore, as the average residence time increases the deviation of yield between the eight-capillary system and the single capillary system decreases. This indicates that the effect of flow distribution deterioration on the numbering-up becomes obviously weaker when the average residence time (reaction time) becomes longer as soon as the flow in the multi-capillary system is still stable enough. That is, slight flow maldistribution will not significantly influence the mass transfer between gas-liquid two phases, the residence time in each capillary and thus the overall reaction performance in the multi-capillary systems. The flow rate distribution (throughput) in each capillary is also analyzed under reaction conditions and compared to the performance in the hydrodynamic study (without reaction). Figure 34 shows the deviation of the throughput among the channels of the particular reactor. It can be seen that the performance under reaction conditions is less good than in the hydrodynamic study (Figure 22); it is because the reaction can lead to system instability which is not good for

flow distribution. However, the deviation is still lower than 10 percent thus the performance is among the best according to literature[30].

It can be concluded that reaction performance slightly decreases when the process of numbering-up is applied, but still similar yield is obtained. Therefore, the process of numbering-up is highly applicable for scale-up of reaction systems.

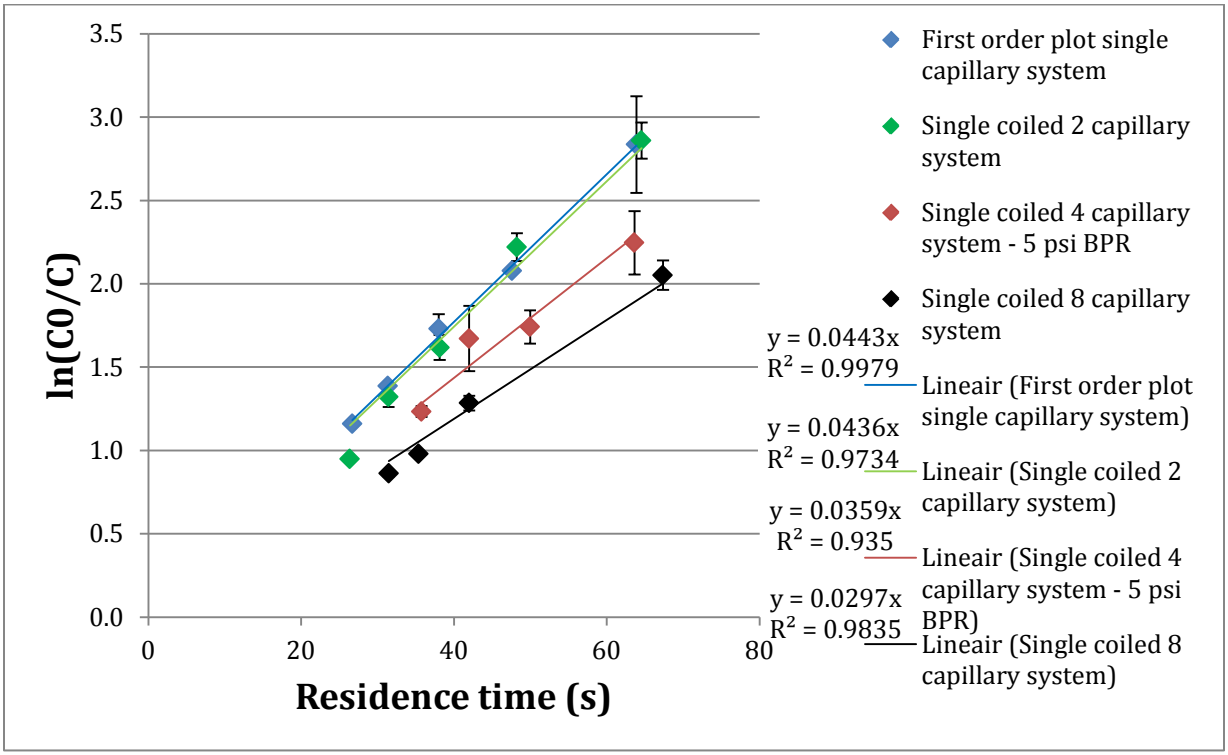

Figure 33: Kinetics in numbered-up reactors

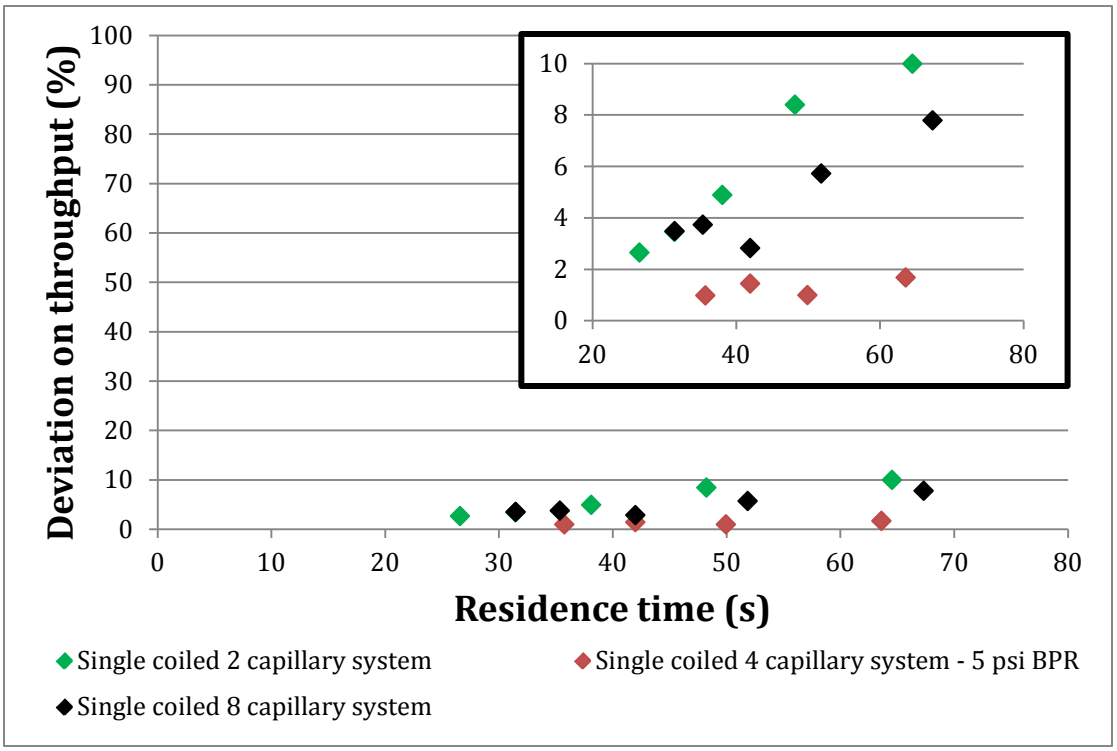

Figure 34: Deviation on throughput of numbered-up reactors

Eight-capillary system

A photo of the set-up for eight-capillary system is shown in Figure 35 for an actual impression of the system. In this figure the mass flow controller (1), syringe pump (2), distributor section (3), reactors (4) and reactor outlets/collector (5) are shown. Also, the distribution of the air cooling can be seen (6), which is split-up via a custom made glass distributor. This photograph can be compared to the schematic representation in Figure 16.

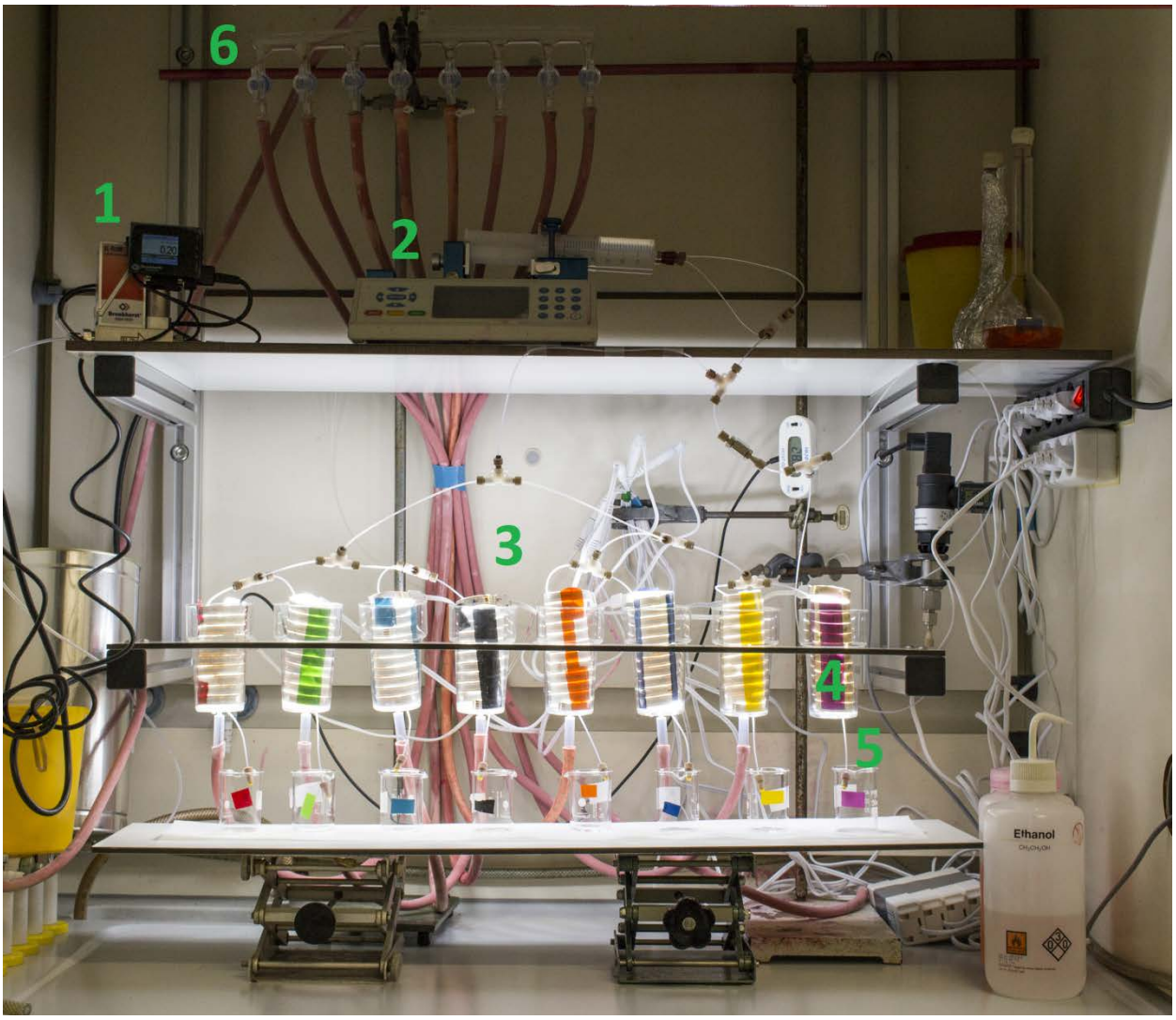

Figure 35: Photo of the eight-capillary set-up

Two-capillary system

Besides these previous mentioned reactor systems also a system with two capillaries and only one light source is tested. If a LED strip can provide a sufficient photon flux for two reaction channels, the system can be more energy efficient. In order to test this, two capillaries are coiled on top of each other (double coiled) with only one light source coiled around this reactor system, as can be seen in Figure 11. The results of this double coiled system are represented in Figure 36, which shows that the double coiled system results in lower yield than the single capillary and the single coiled two-capillary system. Note that both systems have a very small error margin, as can be seen from the error bars in Figure 36. It can be concluded that the reaction system is photon limited in the double coiled set-up. It can also be seen that the yield differs approximately 15 percent from the single coiled system. In Figure 37 the relationship between C0/C and the residence time indicates first order kinetics with respect to thiophenol. This figure shows that in all of the three cases first order kinetics is obtained; however, for the double coiled system the kinetic constant is approximately 40 percent lower. This lower value can be explained by the lower photon flux per channel, thus the lower amount of photons in each channel. Apparently, the photon flux is insufficient to provide both channels with enough photons to reach similar conversions compared to the single coiled system. It can also be concluded that there is a surplus of photons in the single coiled system. Light source optimization can be done on this part, e.g. a more efficient light source could be selected or the length of the light source could be shortened or enlarged according to the capillary length.

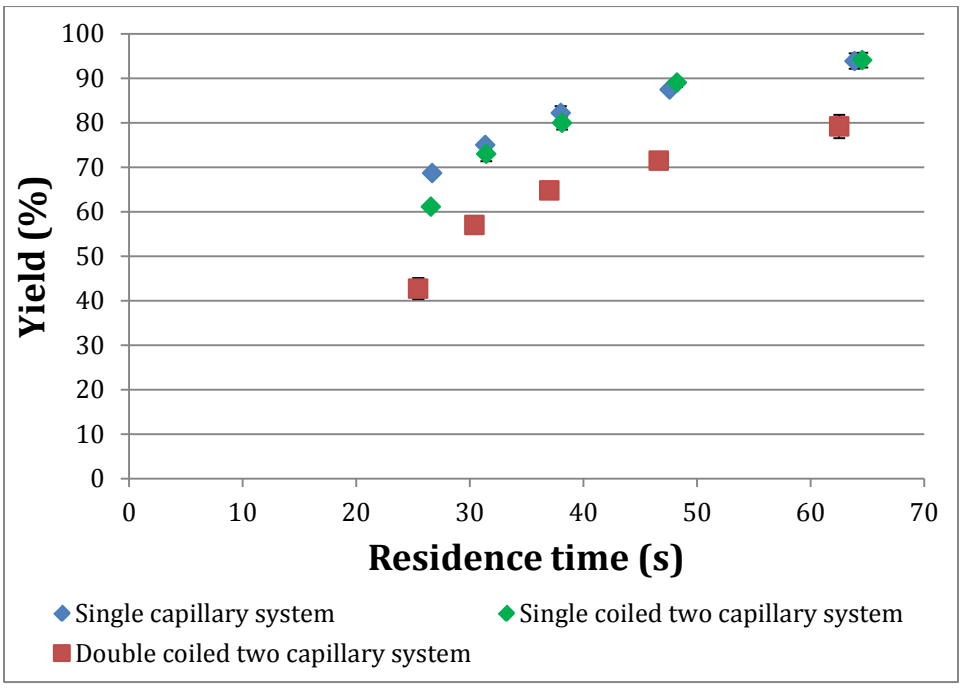

Figure 36: Performance of the double coiled system

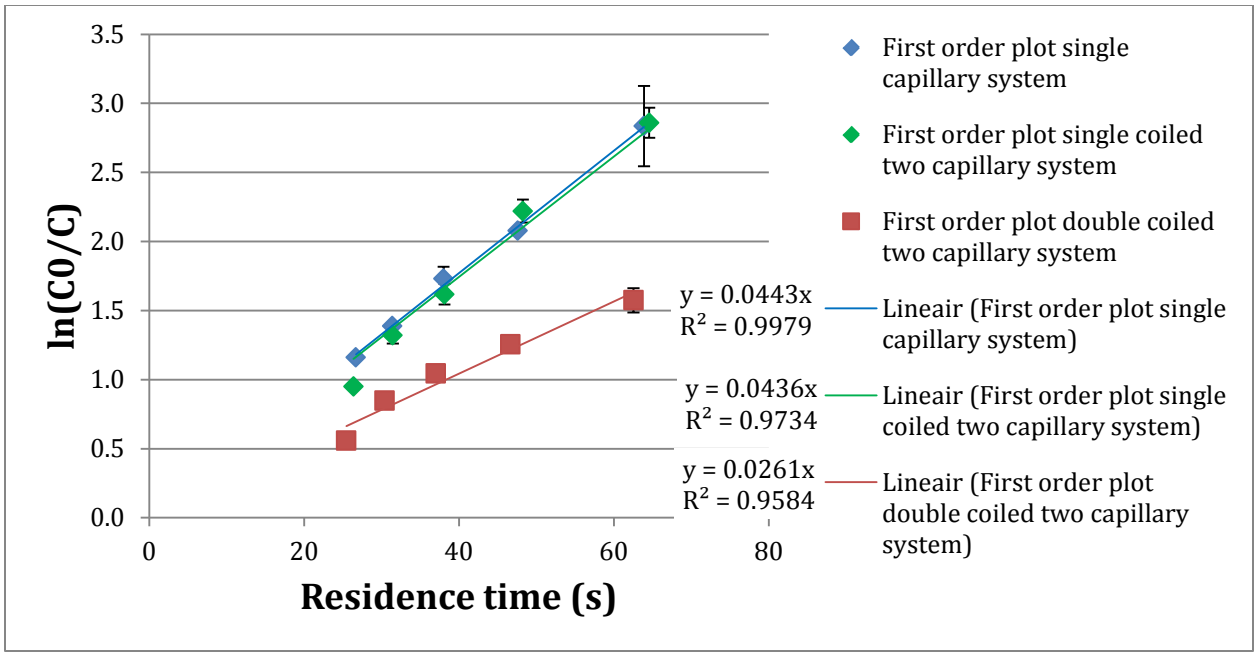

Figure 37: Kinetics of single capillary, single coiled two capillary and double coiled two capillary reactor

4.2.4 Quantum yield

A method for describing the reaction efficiency is by calculating the quantum yield of the reaction system, which is determined as the amount of product normalized with the absorbing species over the amount of photons putted into the system[2], as is stated in Equation (18). In literature quantum yield is already determined for batch experiments[33]. The equation used in literature can be converted to flow experiments, as can be seen in Equation (19). As the model reaction used in this research is first order in thiophenol, it is assumed that only half of the substrate molecules have to be activated for conversion. Then, Equation (20) holds for this system.

$$\varphi = \frac{N_{product}}{N_{photons}} \tag{18}$$

$$\varphi = \frac{C_{product} Q}{q_{p,\lambda}} \tag{19}$$

$$\varphi = \frac{V_r C_0 \varepsilon_{cat} X}{2\tau q_{p,\lambda}} \tag{20}$$

With the curtesy of Robin Verijke, a master student in our group, we were able to determine the average photon flux in the capillary reactors using actinometry[34]. The reaction equation of the actinometer is represented in Figure 38. Except for the photon flux and the irradiation time

every aspect of this equation is known thus making this reaction suitable for determination of the photon flux.

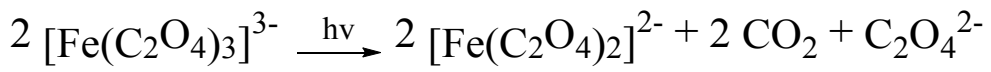

Figure 38: Reaction equation of the actinometer

$$F(X)=\frac{\frac{1}{\varepsilon_\lambda l_\lambda}\ln\left(\frac{1-e^{-\varepsilon_\lambda C^0_{ACT} l_\lambda}}{1-e^{-\varepsilon_\lambda C^0_{ACT}(1-X) l_\lambda}}\right)+C^0_{ACT}X}{\varphi / V_c}=q_{p,\lambda}\tau \qquad (21)$$

Using equation (21) the photon flux ($q_{p,\lambda}$) can be calculated, which results in a photon flux of $2.98\cdot10^{-8}$ einstein/s with a 15 percent error margin. Subsequently, the quantum yield is calculated and plotted versus the conversion, as shown in Figure 39. The graph states that the quantum yield decays with high conversion, as is expected. Because the photon flux is measured with an error margin and the residence time is calculated theoretically also the quantum yield has an error. However, based on these results it can be assumed that the reaction is not a radical chain reaction.

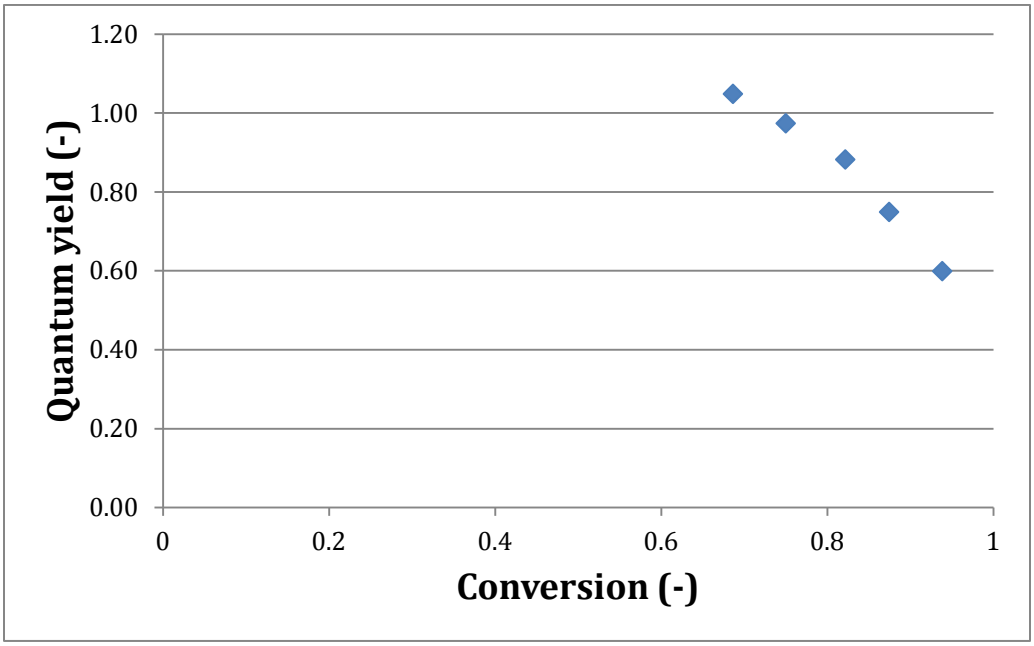

Figure 39: Quantum yield of the model reaction

Chapter 5

Conclusions

In this research two reactor types are evaluated: a chip reactor and a self-designed capillary reactor. The experiments in the chip reactor showed that capillary forces had a significant contribution on the multi-phase flow distribution. This contribution resulted in the fact that good distribution was only obtained at very high flow rates, which implies very low residence times of even less than one second. These results made the application of the selected model reaction impossible, because significant conversion cannot be obtained with such low residence times.

A good alternative is found in the self-designed capillary reactor. Scale-up via numbering-up is established and proved to be successful. The hydrodynamic study showed perfect scale-up properties for liquid throughputs of 0.4 ml/min and higher with a gas to liquid flow rate ratio of 3:1. Deviation of the flow rate among parallel capillaries showed similar results for two, four and eight capillary reactors. Also, the principle of pressure drop difference in the two parts including distributor and parallel capillaries proved to be highly feasible in these type of reactors. Furthermore, the introducing modes of gas and liquid two phases in the T-micromixer where Taylor flow is formed seems to be an important parameter which affect the splitting of flow downstream. It has also been shown that the used capillary or pressure resistance (e.g. BPR) in the section between the T-micromixer and the next T-micromixer used as splitting unit has a significant influence on Taylor flow splitting. Experimental results also show the strategy with separately splitting up gas and liquid flows and then combing gas and liquid flow does not work well in the flow splitting due to the occurrence of circular flow (Figure 23). This proves that the process of splitting up a flow is reactor depended.

Implementation of the model reaction in the best performing systems showed that numbering-up is an excellent technique for scale-up of photocatalytic reactions in microreactors. The obtained yield of the model reaction only slightly decreases with increasing amount of reactors. Moreover, first order kinetics are measured for all reactor systems, which shows the stability of the scale-up procedure. This stability is also proven by a deviation in yield of less than 5 percent and a deviation in throughput of less than 10 percent. Furthermore, it is proven that the configuration of the T-mixer where gas and liquid flow are combined into segmented flow has a significant contribution to the stability of the system. Also there is found that a constant photon flux in each reactor can contribute largely to the stability of the system.

Actinometry allowed to obtain the quantum yield of the model reaction for the single capillary reactor system. The results show that the reaction system can be photocatalytic. Subsequently, a reaction mechanism is proposed based on redox potentials and obtained first order kinetics.

Chapter 6

Recommendations

In this research the principle of numbering-up in a flexible capillary reactor for homogeneous photoredox catalyzed reactions is showed. This research can be improved on two main topics, which are performance optimization of the self-designed multi-capillary system and research that focuses on production application.

However, not much optimization work has been done on this topic. More time could be invested in studying the performance of the 8 channel capillary system while increasing the pressure in the distribution part. Also, the length and diameter of the distribution parts can be varied.

Furthermore, recombination of the 8 outlets can be studied. It would be interesting to see whether recombination would diminish the error in deviation or that circular flow would be obtained, as was the case with one of the 2 capillary set-ups, which is depicted in Figure 23.

Another interesting topic, for application in industry, is to know the performance of the reactor while the reactor is suffering from channel blockage. This can easily be simulated by attaching a stop as replacement for one of the channels. Another form of flow disturbance can occur when one or multiple light sources stop working, this can easily be simulated by disconnecting light sources.

Moreover, the principle and quality of numbering-up could be shown even more by running some tests over a longer period of time. Here for operating times of even multiple days would be suitable[21].

Finely, the flow regime can be evaluated. Literature shows that for some reactions similar yield can be obtained for much higher throughputs by adjusting the flow regime from Taylor flow to annular flow[35]. If the reduced residence time is outweighed by increased contact time between the gas and liquid phase, reactions can take place more efficient. This statement can hold for reaction media that are limited by photon penetration.

Chapter 7

Nomenclature

A	Absorbance	(-)
C	Concentration	$mol \cdot m^{-3}$
C_A	Concentration of species A	$mol \cdot m^{-3}$
C_{ACT}	Concentration of the actinometer	$mol \cdot L^{-1}$
$C_{B,bulk}$	Concentration of species B in the bulk phase	$mol \cdot m^{-3}$
C_λ	Concentration of the light absorbent	$mol \cdot L^{-1}$
Ca	Capillary number	(-)
D_A	Molecular diffusivity of species A	$m^2 \cdot s^{-1}$
E_λ	Energy per wavelength transmitted	W/nm
I	Light intensity	$W \cdot m^{-2}$
k_L	Mass transfer constant	$m \cdot s^{-1}$
$k_{m,n}$	Reaction rate constant	
l_λ	Mean free pathway of light	cm
m	Order of species A	(-)
n	Order of species B	(-)
N	Amount	mol
P	Pressure	Pa
$P_{light\ source}$	Power of the light source	W
Q	Throughput	$m^3 \cdot s^{-1}$
Q_G	Gas throughput	$m^3 \cdot s^{-1}$
Q_L	Liquid throughput	$m^3 \cdot s^{-1}$
$q_{p,\lambda}$	Photon flux	$einstein \cdot s^{-1}$
R	Gas constant	$J \cdot mol^{-1} \cdot K^{-1}$
T	Temperature	K
T_λ	Transmittence	(-)
v	Superficial velocity	$m \cdot s^{-1}$
V_c	Volume of the capillary reactor	m^3
w	Weight fraction	(-)
X	Conversion of the actinometer	(-)
Y	Yield	(-)
γ	Surface tension	$N \cdot m^{-1}$
ε_{cat}	Catalyst loading	$mol_{cat} \cdot mol_{sub}^{-1}$
ε_λ	Absorption coefficient	$L \cdot mol^{-1} \cdot cm^{-1}$
η_{light}	Fraction of energy converted into light	(-)
λ	Wavelength	nm
μ	Dynamic viscosity	Pa·s
σ	Standard deviation	
φ	Quantum yield	$mol \cdot einstein^{-1}$

Chapter 8

Bibliography

1. Hessel, V., Kralisch, D., Kockmann, N., Noël, T. & Wang, Q. Novel process windows for enabling, accelerating, and uplifting flow chemistry. *ChemSusChem* 6**,** 746–789 (2013).

2. Su, Y., Straathof, N., Hessel, V. & Noël, T. Photochemical transformations accelerated in continuous-flow reactors: basic concepts and applications. *Chem. Eur. J.* 20**,** 10562–89 (2014).

3. Gemoets, H., Su, Y., Shang, M., Hessel, V., Luque, R., Noël, T. Liquid phase oxidation chemistry in continuous-flow microreactors. *R. Soc. Chem.*, in publication, (2015).

4. Hessel, V., Angeli, P., Gavriilidis, A. & Lo, H. Gas - Liquid and Gas - Liquid - Solid Microstructured Reactors: Contacting Principles and Applications. *Ind. Eng. Chem. Res.* 44, 9750–9769 (2005).

5. Nijhuis, X. Multiphase Heterogeneous Catalysis in Continuous Flow Microreactors. in (TU/e).

6. Noël, T. & Buchwald, S. Cross-coupling in flow. *Chem. Soc. Rev.* 40, 5010-5029, (2011).

7. Wang, X., Cuny, G. & Noël, T. A Mild, One-Pot Stadler-Ziegler Synthesis of Arylsulfides Facilitated by Photoredox Catalysis in Batch and Continuous-Flow. *Angew. Chemie* 125, 8014–8018 (2013).

8. Wong, P. & Choi, S. K. Mechanisms of Drug Release in Nanotherapeutic Delivery Systems. *Chem. Rev.* 115, 3388–3432 (2015).

9. Jike, L., Yingbei, S., Jingyun, M., Li, D., Fang, W., Tianwei, T. Photochemical production of vitamin D2, scale-up and optimization. *Chem. Eng. Technol.* 30, 261–264 (2007).

10. Reis, N. & Li Puma, G. Novel Microfluidic Approach for Extremely Fast and Efficient Photochemical Transformations in Fluoropolymer Microcapillary Films. *Chem. Commun.* 51, 8414–8417 (2015).

11. Talla, A., Driessen, B., Straathof, N., Milroy, L., Brunsveld, L., Hessel, V., Noël, T. Metal-Free Photocatalytic Aerobic Oxidation of Thiols to Disulfides in Batch and Continuous-Flow. *Adv. Synth. Catal.* 357, 2180–2186 (2015).

12. Su, Y., Hessel, V., Noël, T. A compact Photomicroreactor Design for Kinetic Studies of Gas-Liquid Photocatalytic Transformations. *Am. Inst. Chem. Eng.* 61, 2215–2227 (2015)..

13. Kockmann, N., Gottsponer, M. & Roberge, D. Scale-up concept of single-channel microreactors from process development to industrial production. *Chem. Eng. J.* 167**,** 718–726 (2011).

14. Roberge, D., Gottsponer, M., Eyholzer, M. & Kockmann, N. Industrial design, scale-up, and use of microreactors. *Chim. Oggi* 27**,** 8–11 (2009).

15. Al-Rawashdeh, M., Fluitsma, L., Nijhuis, T., Rebrov, E., Hessel, V., Schouten, J. Design criteria for a barrier-based gas-liquid flow distributor for parallel microchannels. *Chem. Eng. J.* 181-182, 549–556 (2012).

16. Al-Rawashdeh, M., Yu, F., Nijhuis, T., Rebrov, T., Hessel, V., Schouten, J. Numbered-up gas-liquid micro/milli channels reactor with modular flow distributor. *Chem. Eng. J.* 207-208, 645–655 (2012).

17. Su, Y., Chen, G. & Kenig, E. An experimental study on the numbering-up of microchannels for liquid mixing. *Lab Chip* 15, 179-187 (2015).

18. Guo, X., Fan, Y., Luo, L. Mixing performance assessment of a multi-channel mini heat exchanger reactor with arborescent distributor and collector. *Chem. Eng. J.* 227, 116–127 (2013).

19. Mendorf, M., Nachtrodt, H., Mescher, A., Ghaini, A. & Agar, D. Design and Control Techniques for the Numbering-up of Capillary Microreactors with Uniform Multiphase Flow Distribution. *Ind. Eng. Chem. Res.* 49, 10908–10916 (2010).

20. Schenk, R., Hessel, V., Hofmann, C., Kiss, J., Löwe, H., Ziogas, A. Numbering-up of micro devices: a first liquid-flow splitting unit. *Chem. Eng. J.* 101, 421–429 (2004).

21. Iwasaki, T., Kawano, N. & Yoshida, J. Radical polymerization using microflow system: Numbering-up of microreactors and continuous operation. *Org. Process Res. Dev.* 10, 1126–1131 (2006).

22. Zhao, Y., Chen, G. & Yuan, Q. Liquid – Liquid Two-Phase Mass Transfer in the T-Junction Microchannels. *Am. Inst. Chem. Eng.* 53, 3042–3053 (2007).

23. Zhao, Y., Chen, G. & Yuan, Q. Liquid-Liquid Two-Phase Flow Patterns in a Rectangular Microchannel. *Am. Inst. Chem. Eng.* 52, 4052–4060 (2006).

24. Kashid, M. N., Gupta, A., Renken, A., Kiwi-Minsker, L. Numbering-up and mass transfer studies of liquid–liquid two-phase microstructured reactors. *Chem. Eng. J.* 158, 233–240 (2010).

25. Chen, J., Wang, S., Ke, H., Cai, S., Zhao, Y. Gas-liquid two-phase flow splitting at microchannel junctions with different branch angles. *Chem. Eng. Sci.* 104, 881–890 (2013).

26. Fu, T. & Ma, Y. Bubble formation and breakup dynamics in microfluidic devices: A review. *Chem. Eng. Sci.* , in publication, (2015).

27. Kim, S., Yong, S. Split of two-phase plug flow with elongated bubbles at a microscale branching T-junction. *Chem. Eng. Sci.* 134, 119–128 (2015).

28. Yue, J., Boichot, R., Luo, L. & Gonthier, Y., Chen, G. & Yuan, Q. Flow Distribution and Mass Transfer in a Parallel Microchannel Contactor Integrated with Constructal Distributors. *Am. Inst. Chem. Eng.* 56, 298–317 (2010).

29. Chen, J., Wang, S., Zhang, X., Ke, H., Li, X. Experimental investigation of two-phase slug flow splitting at a micro impacting T-junction. *Int. J. Heat Mass Transf.* 81, 939–948 (2015).

30. Al-Rawashdeh, M. & Nijhuis, X., Rebrov, E., Hessel, V. & Schouten, J. Design Methodology for Barrier-Based Two Phase Flow Distributor. *Am. Inst. Chem. Eng.* 58, 3482–3493 (2012).

31. Al-Rawashdeh, M., Zalucky, J., Müller, C., Nijhuis, T., Hessel, V. & Schouten, J. Phenylacetylene hydrogenation over [Rh(NBD)(PPh_3)$_2$]BF_4 catalyst in a numbered-up microchannels reactor. *Ind. Eng. Chem. Res.* 52, 11516–11526 (2013).

32. Wang, X., Zhu, C., Fu, T. & Ma, Y. Bubble Breakup with Permanent Obstruction in an Asymmetric Microfluidic T-Junction. *Am. Inst. Chem. Eng.* 61, 1081-1091 (2015).

33. Cismesia, M. & Yoon, T. Characterizing Chain Processes in Visible Light Photoredox Catalysis. *Chem. Sci.*, in publication, (2015).

34. Aillet, T., Loubiere, K., Dechy-Cabaret, O. & Prat, L. Accurate Measurement of the Photon Flux Received Inside Two Continuous Flow Microphotoreactors by Actinometry. *Int. J. Chem. React. Eng.* 12, 1–13 (2014).

35. De Mas, N., Günther, A., Schmidt, M. & Jensen, K. Increasing productivity of microreactors for fast gas-liquid reactions: The case of direct fluorination of toluene. *Ind. Eng. Chem. Res.* 48, 1428–1434 (2009).

36. Romero, N. & Nicewicz, D. Mechanistic Insight into the Photoredox Catalysis of Anti- Markovnikov Alkene Hydrofunctionalization Reactions. *J. Am. Chem. Soc.* 136, 17024–17035 (2014).

37. Hari, D. P. & König, B. Synthetic applications of eosin Y in photoredox catalysis. *Chem. Commun. (Camb).* 50, 6688–99 (2014).

38. Wood, P. The potential diagram for oxygen at pH 7. *Biochem. J.* 253, 287–289 (1988).

39. Kirihara, M., Asai, Y., Ogawa, S., Noguchi, T., Hatano, A., Hirai, Y. A mild and environmentally benign oxidation of thiols to disulfides. *Synthesis (Stuttg).* 21, 3286–3289 (2007).

40. Amat-Guerri, F., López-González, M., Martínez-Utrilla, R. & Sastre, R. Singlet oxygen photogeneration by ionized and un-ionized derivatives of Rose Bengal and Eosin Y in diluted solutions. *J. Photochem. Photobiol. A Chem.* 53, 199–210 (1990).

Appendix I

The photocatalytic cycle is still not known. Therefore, the mechanism is studied via analysis of redox potentials resulting in a proposed mechanism. It should be noted that the redox potentials are estimations as they are dependent on parameters such as solvent and pH. These redox potentials are obtained from literature[36–38]. There should also be mentioned that previous work in our group showed that the formation of phenyl disulfide neither occurs in the absence of the catalyst or oxygen. Then the catalytic cycle can be composed based on redox potentials, which can be seen in Figure 40. This figure shows the most likely pathway based on redox potentials.

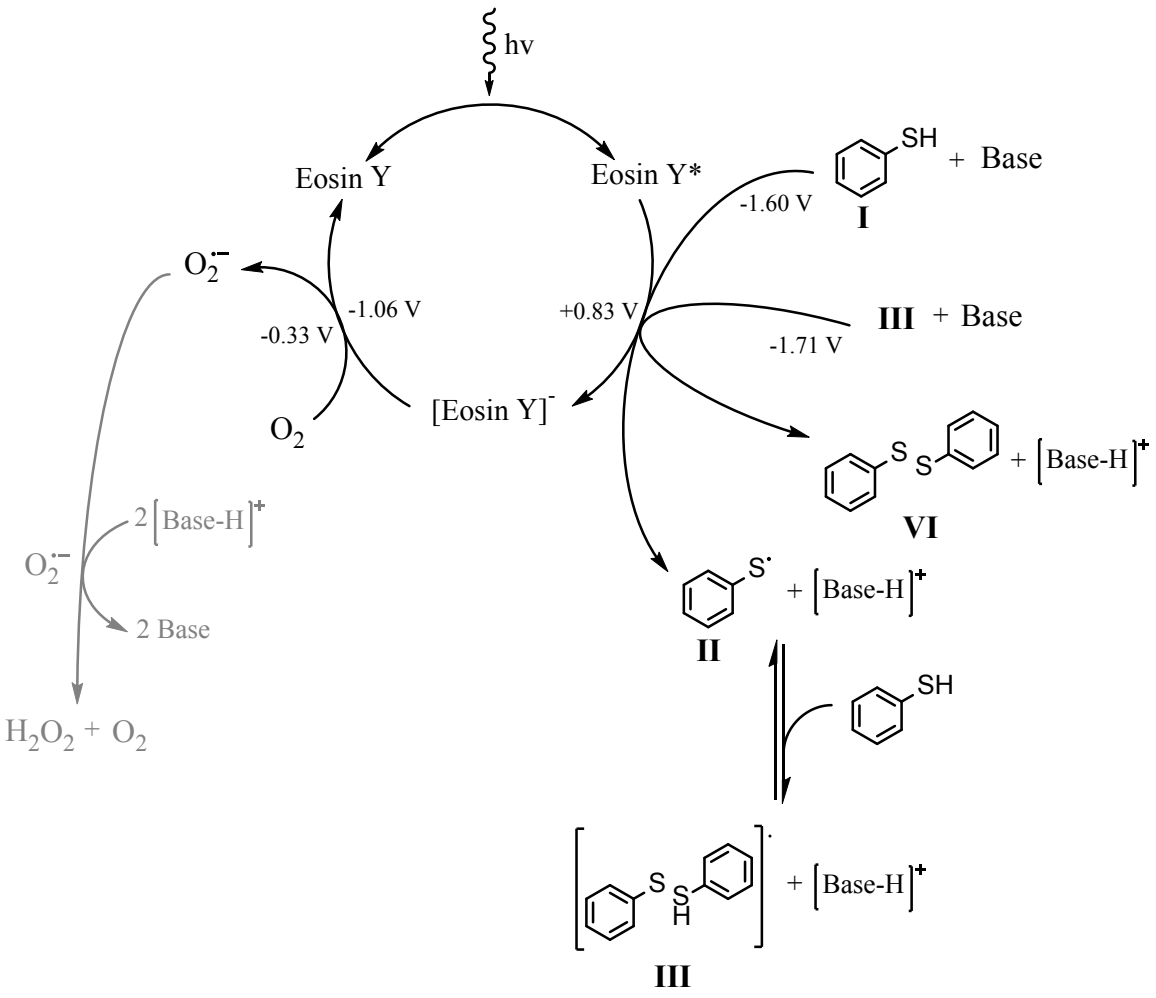

Figure 40: Proposed mechanism of phenyl disulfide formation

As can be seen above, the superoxide, which is not very stable, can form hydrogen peroxide with the protons on the base. Hydrogen peroxide can also catalyze the reaction; however, the kinetics indicate no significant contribution of hydrogen peroxide to the reaction order. This insignificant contribution is probably due to a slow reaction rate of the hydrogen peroxide

catalyzed reaction under these circumstances. A low reaction rate for this reaction is also observed in literature[39]. The formed hydrogen peroxide will eventually degrade into water and oxygen, as previous work showed no presence of hydrogen peroxide in the product mixture.

Alternative pathways

Other pathways should be discussed as well. Besides the proposed mechanism there are two alternatives. The first alternative is reaction via singlet oxygen as a catalyst; however, the singlet oxygen to the superoxide ion only has a redox potential of +0.65 V, which is less than the reduction of the exited Eosin Y (+0.83 V) as showed in the proposed mechanism. There can be assumed that the above mechanism is favored. It is also known that Eosin Y is not a good singlet oxygen promoter with a quantum yield of approximately 0.32[40]. The second alternative, is that the intermediate product (III) in Figure 40 is converted to the product (IV) via the reduction of oxygen to the superoxide ion. Simultaneously, oxygen can also oxidize the reduced Eosin Y species thus resulting in two superoxide ions. These two ions can, in combination with the protonated base, form hydrogen peroxide. However, the redox potential of the reduction of oxygen to the superoxide ion is only -0.33 V whereas the redox potential of the redox potential of the reduction of the excited Eosin Y species is +0.83 V. Again it can be assumed that the proposed mechanism will be favored as the potential difference of the formation of the product (IV) from the intermediate product (III), -1.71 V, is larger.

Acknowledgements

I would gladly like to thank my daily supervisor Yuanhai Su, my supervisor Timothy Noël and my graduation professor Volker Hessel for giving me the opportunity to conduct this research in the SCR-sfp group. I really enjoyed the graduation period and I have learned a lot about engineering. I also would like to thank my parents for their continuous support during my studies and all the choices that I have made: this is really valuable to me.

Now I would like to thank some of the group members in particular. Timothy for all the good feedback that I have received and for the confidence of letting me design my own reactor. Yuanhai for all the good discussion that we had and for always being there for answering all the questions that I had. I also want to thank Nico for all the fruitful discussions that we had and for all the consulting hours that you have put into my research. I think that, next to being a chemist, you will be a perfect engineer in the future. One last advice: don't work at high pressures. I would like to thank Natan in particular for his contribution in proposing the mechanism, but also for the funny moments when he fooled people (je zal wel denken nu: "Goed verhaal dit, lekker kort ook."). Thanks to Hannes for the nice carnival drink: yes Hannes, it was nice. Also I would like to thank the Italian people: Dario and Ceci even though you arrived later you guys really increased the atmosphere in the group. There was never a dull moment with you.
Last but not least I insist to thank my fellow students during this graduation project, Patricia and Robin, we discussed a lot about all our projects, but more importantly with you guys it was always a pleasure to come to the university. Now I don't know if I have to thank Robin for showing his dancing skills or not…
I will never forget one thing though: Eosin Y can make everything pink. Yuanhai can confirm that. When he blew up his stock solution his whole fume hood turned pink and he had to put in several hours to clean it.

Thanks to all of you, I really enjoyed it.